Science of the Total Environment 912 (2024) 169112

Contents lists available at ScienceDirect

Science of the Total Environment

journal homepage: www.elsevier.com/locate/scitotenv

Is ebullition or diffusion more important as methane emission pathway in a shallow subsaline lake?

Pamela Alessandra Baur [a,b,*], Daniela Henry Pinilla [a,1], Stephan Glatzel [a,b]

[a] University of Vienna, Faculty of Earth Sciences, Geography and Astronomy, Department of Geography and Regional Research, Working group Geoecology, Josef-Holaubek-Platz 2, Vienna 1090, Austria
[b] University of Vienna, Faculty of Life Sciences, Vienna Doctoral School of Ecology and Evolution (VDSEE), Djerassiplatz 1, Vienna 1030, Austria

HIGHLIGHTS

- Higher median CH_4 fluxes via diffusion compared to ebullition at Lake Neusiedl.
- Acetoclastic methanogenesis is the dominant CH_4 production type at Lake Neusiedl.
- Highest (mean) CH_4 fluxes occur at the *Reed belt* site, irrespective of the pathway.
- In the *Reed belt*, ebullition contributes 48 % to the total cumulative CH4 emission.
- In the *Channel* and *Open water/Lake* locations, ebullition accounts for only about 1 %.

GRAPHICAL ABSTRACT

The contribution and dominance of CH_4 emissions from the ebullition and the diffusion pathway of a shallow subsaline lake was investigated at three representative locations (*Channel, Reed belt, Open water/Lake*) at Lake Neusiedl.

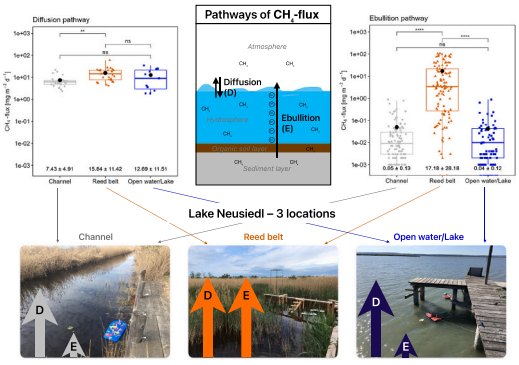

ARTICLE INFO

Editor: Jurgen Mahlknecht

Keywords:
CH_4 emissions
Bubble flux
Phragmites australis
Stable carbon isotope
Lake Neusiedl
Methanogenesis

ABSTRACT

Methane (CH_4) emissions via ebullition contribute significantly to greenhouse gas emissions from freshwater bodies. According to the literature, the ebullition pathway may even be the most important pathway in some cases, particularly in shallow lakes. Ebullition rates are not often estimated because of the high uncertainty associated with episodic releases, leading to difficulties in their determination. This study provides an estimate of such emissions in a large, shallow, subsaline lake in eastern Austria, Lake Neusiedl, and compares them to the diffusion pathway. Ebullition gas sampling was conducted every 5–10 days over a period of 107 days from late March to mid-July 2021, using ebullition traps placed in three distinct locations: *Reed belt*, *Channel* and *Open water/Lake*. The aim was to study the temporal and spatial heterogeneity of ebullition and its contribution to total emissions. At the same time, several water quality and other environmental parameters were measured and then tested against the CH_4 ebullition rates to explore them as potential drivers for this pathway. The carbon isotope fractionation factor (α_C) of the measured CH_4 ebullition gas, ranging from 1.03 to 1.06, indicates a dominance of the acetoclastic methanogenesis in the sediments of Lake Neusiedl, regardless of the location. The

* Corresponding author.
E-mail addresses: pamela.baur@univie.ac.at (P.A. Baur), dhenry@icra.cat (D. Henry Pinilla), stephan.glatzel@univie.ac.at (S. Glatzel).
[1] Present address: Catalan Institute for Water Research (ICRA), Department of Resources and Ecosystems, Carrer Emili Grahit 101, Girona, 17003, Catalonia, Spain.

https://doi.org/10.1016/j.scitotenv.2023.169112
Received 4 September 2023; Received in revised form 11 November 2023; Accepted 2 December 2023
Available online 8 December 2023

Reed belt location showed the highest mean CH_4 ebullition rate (17 ± 28 mg CH_4 m^{-2} d^{-1}), which is >340-fold higher than the mean of the other two locations, and demonstrated also a strong temperature dependency. In all locations at Lake Neusiedl, the median CH_4 fluxes via diffusion are significantly higher than via ebullition. Our analyses do not confirm the dominance of the ebullition pathway in any of the studied locations. Whereas at the *Reed belt*, ebullition accounts for 48 % of the CH_4 emissions, in the other two locations, is responsible only for about 1 %.

1. Introduction

Lakes cover only around 1.8–2.2 % of the earth's land surface (Pi et al., 2022; Messager et al., 2016), nevertheless, they emit yearly on average 151 ± 73 Tg (mean ± 95 % CI) of methane (CH_4), accounting for about 35 % of the total aquatic and about 19 % of the global CH_4 emissions (Rosentreter et al., 2021). Lakes are natural sources of CH_4, where its production (methanogenesis) occurs mainly in anoxic sediments by methanogenic archaea (methanogens). Globally, more than half of all large lakes (53 %, including Lake Neusiedl) have decreased in water volume over the last three decades (1992–2020) due to anthropogenic and climatic drivers such as higher water consumption or higher evaporation rates (Yao et al., 2023). Saline lakes, which represent a significant portion of all lakes in terms of both volume (44 %) and area (23 %) (Messager et al., 2016), also showed a strong decline (Wurtsbaugh et al., 2017). This is particularly concerning since several biogeochemical processes that occur within lakes play a fundamental role in the global carbon (C) cycle, such as primary production, sedimentation and burial, lateral transport, and exchange with the atmosphere (Alin and Johnson, 2007).

CH_4 is a powerful greenhouse gas (GHG), with a 96 times higher Sustained-Flux Global Warming Potential (SWGWP) than carbon dioxide (CO_2) over a 20-years time horizon on a mass basis (Neubauer and Megonigal, 2015). Therefore, it is of major significance to study in detail the quantity, frequency and distribution of CH_4 fluxes in lake ecosystems.

Methanogenesis can be classified into three different types (also referred in the literature as methanogenic pathway) according to the main substrate that methanogens consume for CH_4 production. These types are: acetoclastic (acetate), hydrogenotrophic (hydrogen plus CO_2) or methylotrophic (methyl-compounds). According to Whiticar (1999), the hydrogenotrophic methanogenesis is the dominant metabolism of CH_4 production in marine ecosystems and the acetoclastic methanogenesis is more relevant in freshwater ecosystems. Methylotrophic methanogenesis is widespread in saline environments, but its proportion is considered to be lower than the other two methanogenesis types because of the smaller amount of substrate available for consumption (Conrad, 2020). In consequence, the methylotrophic methanogenesis is often neglected in many environmental studies.

Stable carbon isotopes are used to trace the sources of CH_4 production and its transformation through CH_4 oxidation and transportation (Conrad, 2005). The carbon isotope fractionation factor (α_C, Eq. (4) in Section 2.3) determines the degree of isotopic discrimination between the reactant (CH_4) and product (CO_2) molecules (Whiticar et al., 1986) and is used to characterize environments based on their dominant methanogenesis type and the transformation due to CH_4 oxidation. Whiticar et al. (1986) showed that α_C differs between freshwater and marine ecosystems, and that it is related to the major methanogenic mechanism. For example, if α_C fluctuates between 1.055 and 1.09, hydrogenotrophic methanogenesis is considered to be the dominant methanogenic mechanism, while α_C values between 1.04 and 1.055 indicate that acetoclastic methanogenesis is the dominant source of CH_4 production. Stable carbon isotopes are further used to detect CH_4 oxidation in lakes (Miller et al., 2022; Bastviken et al., 2002), because CH_4 oxidation enriches the δ^{13}C-CH_4 value (Chanton, 2005). CH_4 oxidation occurs mainly at the anoxic-oxic interface (e.g., water-sediment interface) and is carried out by methanotrophic bacteria (Conrad, 2009).

Once produced, CH_4 can be transported from the anoxic sediment layers to the atmosphere through different pathways, including ebullition (bubble flux released directly and rapidly from sediments), molecular diffusion at the water-air or sediment-air interface, and plant-mediated transport of vascular plants such as *Phragmites australis* (Butterbach-Bahl et al., 2011). The relative importance of each transport pathway varies according to the organic content, the seasonal variation of temperature, and the type and density of vascular plants (Chanton, 2005), as well as the limnobathymetry and the lake morphology (Li et al., 2020).

Ebullition can become the preferential pathway in certain lakes (Aben et al., 2017; Wang et al., 2021a, 2021b; Peeters et al., 2019; Bastviken et al., 2011; Sø et al., 2023), but its dominance is still uncertain due to its high temporal and spatial heterogeneity, and the consequent difficulty to quantify it accurately (Wik et al., 2016; Saunois et al., 2020; Zheng et al., 2022). In global data sets, ebullition was found to be the dominant pathway in (freshwater) lakes, ranging from 56 to 80 % of CH_4 emissions, depending on the approach (DelSontro et al., 2018; Zheng et al., 2022; Bastviken et al., 2011; Johnson et al., 2022). Especially subsaline lakes (salinity 0.5–3 ‰; Hammer (1986)) have often been excluded from global CH_4 estimates due to a lack of observations. Hence, there is a need for more accurate and continuous CH_4 ebullition measurements across different lake ecosystems to reduce the uncertainty in lake methane budgets (Saunois et al., 2020).

Bubble formation occurs because CH_4 is only slightly soluble in water (Yamamoto et al., 1976). Since no reaction with the oxygenated water column takes place during ebullition, at least in shallow waters, and the methanotrophic region in the sediments is bypassed (Happell et al., 1994), no isotopic fractionation takes place during ebullition. This implies that by measuring the δ^{13}C-CH_4 value of the bubbles, conclusions can also be drawn about the main CH_4 production type in the sediments (Chanton, 2005). The bubbles are mainly built up by CH_4 and nitrogen (N_2), whereas other gases like CO_2 account for <1 %, and thus, they can be considered negligible (Langenegger et al., 2019).

Diffusion is one of the other pathways of the CH_4 flux occurring at the sediment-water, water-air or sediment-air interfaces. Diffusion rates are regulated by the concentration gradient, the diffusion coefficient, and the porosity of soil/sediments (Chanton, 2005). Besides CH_4 production, variations in the extent of CH_4 oxidation appear to be the main factor controlling the δ^{13}C-CH_4 value of CH_4 emitted via diffusion (Happell et al., 1994). Peeters et al. (2019) found that in shallow waters, the diffusive CH_4 fluxes from the upper sediments are the main source of dissolved CH_4 in lakes and reservoirs, and of diffusive CH_4 emissions from the water to the atmosphere, rather than CH_4 derived from oxic methanogenesis in the water column as hypothesized by Bogard et al. (2014). Lateral transport can be a possible process causing CH_4 relocation from shallow water zones (site of CH_4 production) to deeper water zones of a lake and, thus, is a main source of diffusive CH_4 emissions from open water of lakes (Encinas Fernández et al., 2016). Globally, the diffusion pathway can account for about 21–25 % of total CH_4 emissions from (freshwater) lakes (Zheng et al., 2022; DelSontro et al., 2018), from which >84 % would be contributed by lakes with an average depth of <5 m (Li et al., 2020).

Until now, ebullition has primarily been studied in freshwater lakes, such as thermokarst (Wang et al., 2021b), boreal and subarctic (Schenk et al., 2021; Wik et al., 2020, 2014, 2013), northern temperate

(Thottathil and Prairie, 2021), tropical (Miller et al., 2022; Linkhorst et al., 2020), and small lakes or reservoirs (McClure et al., 2020; Langenegger et al., 2019; Sø et al., 2023), as well as in urban inland waters (Wang et al., 2021a). However, it has not been comprehensively studied in large shallow and subsaline lakes like Lake Neusiedl. Understanding ebullition in subsaline lakes is crucial. These ecosystems are often shallow (ebullition is restricted to <3 m depth, according to DelSontro et al. (2016)) and if they have a salinity between 0.5 and 5 ‰, they can have the highest (and most variable) CH_4 emissions as known from marshes (Poffenbarger et al., 2011). Subsaline lakes are found across the globe (from Argentina to Greenland) and are often highly sensitive to hydrological and climatic changes (Soja et al., 2013).

Large lakes (>100 km^2) account only for 0.05 % of the total numbers of lakes, but cover 59 % of the total lake area (Pi et al., 2022). Therefore, it is highly important to improve accuracy in the quantification of CH_4 ebullition rates in such large lake ecosystems for more accurate global up-scaling CH_4 emission estimates. Lake Neusiedl, the site of our study, is one of these lakes.

Lake Neusiedl has a surface area of around 315 km^2 and more than half of it is covered by a reed belt dominated by *Phragmites australis* (Wolfram and Herzig, 2013). Due to its unique landscape, it is a cross-border UNESCO world heritage site, a National Park, and a wetland of international importance (Ramsar site) on the Austrian-Hungarian border. Lake Neusiedl is characterized by its subsalinity (Hammer (1986); dominating salt: soda), alkalinty (pH > 8, Reif et al. (2022)), high inorganic turbidity (Zoboli et al., 2023), moderate eutrophication (Tolotti et al., 2021), shallowness (maximum water level of 1.8 m, Wolfram and Herzig (2013)), and by no natural outlet. Due to its shallowness, the high evapotranspiration rates – caused by strong winds and high temperatures – and its dependency on 79 % water input from direct precipitation, Lake Neusiedl is highly sensitive to any climatic change (Soja et al., 2013).

First attempts to investigate the CH_4 fluxes at Lake Neusiedl were conducted by Soja et al. (2014). They measured diffusive CH_4 fluxes using floating chambers during six sampling days in 2011/2012, and did not use a separate methodology for measuring CH_4 ebullition. Furthermore, they did not include the ebullition pathway in the estimated lake's CH_4 budget because of the sporadic release of ebullition. With this approach, they found that 2/3 of the up-scaled lake's diffusive CH_4 fluxes were originated in the reed belt and 1/3 in the pelagic zone. To complement these findings, our study focuses on CH_4 ebullition rates and their significance in comparison to the diffusive CH_4 fluxes in three representative lake ecosystem types of Lake Neusiedl.

To enhance comprehension of the spatial and temporal distribution of CH_4 ebullition, it is essential to identify the sources of CH_4 production and the factors driving ebullition in various lake ecosystems. This is crucial for improving estimates of the CH_4 budget, and exceptionally important given the particular vulnerability of shallow lakes to the impacts of climate variations (Soja et al., 2013; Aben et al., 2017). The objectives of this study are to (1) investigate the spatial and temporal heterogeneity of CH_4 ebullition at the shallow and subsaline Lake Neusiedl, (2) determine the carbon source for methanogenesis based on isotopic ratios of CH_4 from ebullition, (3) explore the drivers of CH_4 ebullition, and (4) compare the ebullition and diffusion pathways in this lake ecosystem. Clarification of these points will help answering the question whether ebullition or diffusion is more important as CH_4 emission pathway in shallow subsaline lakes, using Lake Neusiedl, a site of international importance, as an example.

2. Methods

2.1. Study site and setup

Lake Neusiedl (Fertő, in Hungarian) is the westernmost "steppe" lake in Central Europe without natural outlets, and the only existing artificial outlet has been closed since April 2015 due to low water levels of the lake. The region of Lake Neusiedl holds the status of a transnational UNESCO world heritage site due to its diverse and unique (cultural) landscape. Lake Neusiedl, located on the Austrian-Hungarian border, is a subsaline shallow lake with more than half of its surface covered by a reed belt (181 km^2, Csaplovics (2019)). The reed belt is a dynamically changing mosaic of reed (*Phragmites australis*), water and sediment patches (Buchsteiner et al., 2023), and it is the second largest coherent reed ecosystem in Europe, following the Danube Delta. Especially in 2021, when our ebullition study also took place, intra-annual changes in the mosaic of the reed belt were evident due to the sharp decrease in water areas and the associated overgrowth of the former water pool areas with reeds (Buchsteiner et al., 2023). Our study was conducted on the eastern reed belt of Lake Neusiedl, near the Biological Station Illmitz in Austria (116 m asl, Lat. 47.769° N, Long. 16.758° E, see Fig. 1) in the "nature (core) zone" of the National Park "Neusiedler See - Seewinkel". The region has a mean annual air temperature of 11.1 °C and an annual precipitation of 556 mm (1971–2020) (Hackl and Ledolter, 2023).

Three distinct locations were carefully chosen within the study site, which represent the typical lake ecosystem types of Lake Neusiedl: Channel (CH), Reed belt (RB) and Open water/Lake (OW). These specific locations were selected to represent the spatial variability over the study area and because of their significant differences in water quality (see Table 1) and environmental conditions, such as vegetation cover and wind influence. CH represents the man-made channels in the reed belt, extending from open water to the landward side, often serving as waterways from the open lake to harbors and are, therefore, often maintained. Their lateral exchange with open lake water varies depending on the lake water level, wind direction and wind speed. Location RB represents the water pool areas within the reed belt, characterized by humic-rich, clear and very shallow water and are (almost) not in exchange with lake water. OW represents the open lake water area, which, although it is not far from the edge of the reed belt, shares similar water levels and water characteristics and experiences high turbidity as in the middle of the lake. This area is significantly influenced by strong winds and waves and is particularly exposed to the main wind direction northwest as well as open to the south, which means that OW does not receive shade or wind protection from reeds.

2.2. Methane measurements

Field measurements of the study started in spring (30 March 2021) and ended in early summer (14 July 2021). This study period was chosen to enhance our understanding of CH_4-related processes in a reed-influenced and subsaline lake ecosystem, during a period of rising temperature when reeds start to grow (from dormancy to maturity, see Buchsteiner et al. (2023)) and reach their maximum growth (and subsequent increment in rhizo-deposition). The focus of this study is on the ebullition pathway of CH_4, but for comparison purposes the diffusion pathway was also measured. Two different methodologies were applied for measuring the two CH_4 emission pathways and are described in the following subsections.

2.2.1. Ebullition pathway with ebullition traps

The measurement period for ebullition covered a total of 107 days, during which ebullition gas collection frequency ranged between 5 and 10 days (closure time for the ebullition traps) depending on transport and equipment availability. A total of 14 ebullition gas collection days were registered over the entire study period (15 weeks in total).

At each location (CH, RB, OW), three ebullition traps were permanently installed for gas collection. These traps were built using a floating body-board (approx. 91 cm × 44 cm, Hot Tuna, SportsDirect.com Retail Ltd., UK) equipped with three inverted 23.5 cm diameter HDPE funnels (Emil Lux GmbH & Co. KG, Wermelskirchen, Germany) pierced through. Thus, each location had 9 simultaneous ebullition measurements (funnels). Each funnel was topped with a 50 mL PP syringe featuring a luer lock connector (Omnifix, B. Braun SE, Melsungen, Germany) and

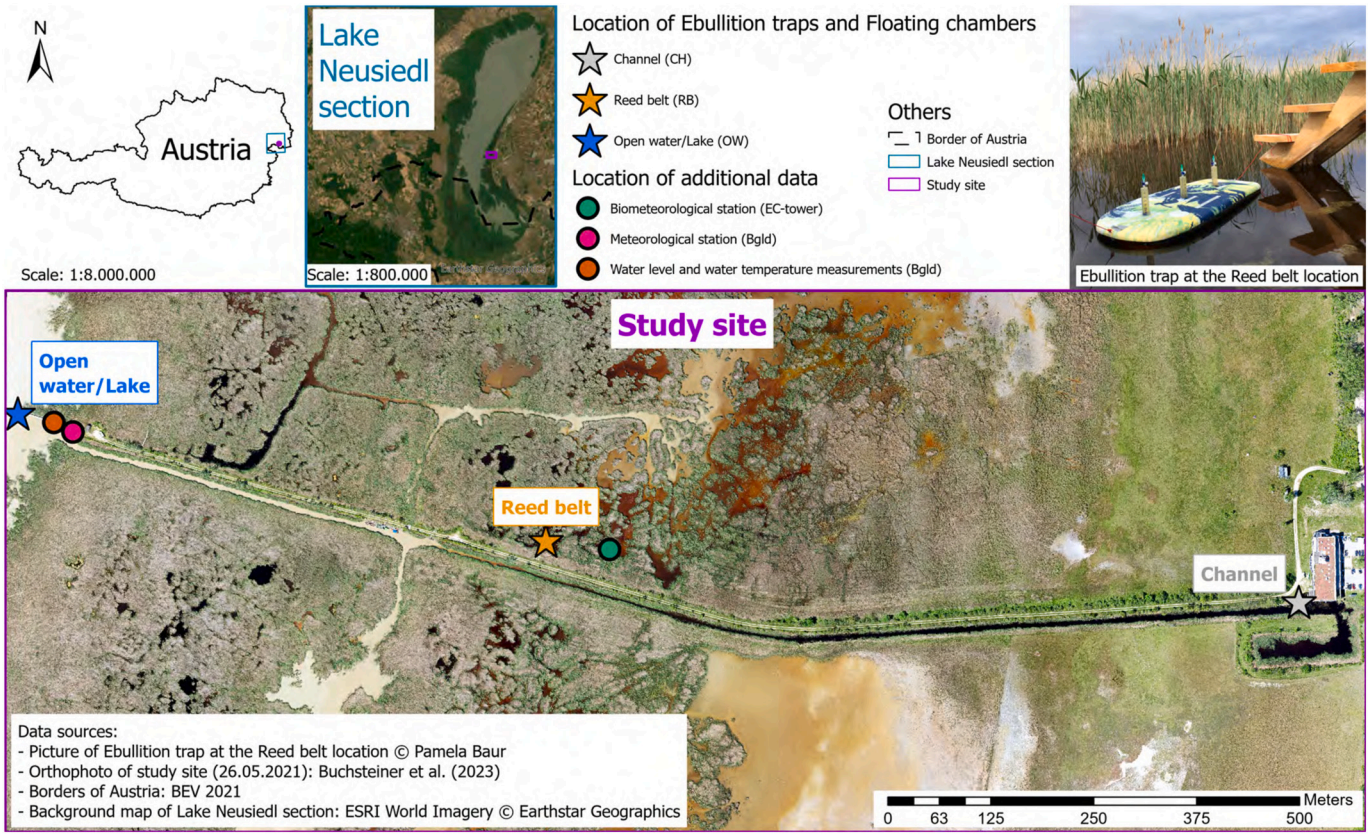

Fig. 1. Geographic location of the study site and monitoring locations of ebullition traps and floating chambers at the reed belt of Lake Neusiedl, near Illmitz, Austria. (Map source: Buchsteiner et al. (2023)).

Table 1
Spatial variability of water characteristics at Lake Neusiedl, illustrated using selected water parameters of three representative locations (CH = Channel; RB = Reed belt; OW = Open water/Lake) prior to the start of the measurement campaign in mid-March 2021 (WL = water level; T_{water} = water temperature; DO = dissolved oxygen; EC = electrical conductivity; TDN = total dissolved nitrogen; NPOC = dissolved non-purgeable organic carbon).

Location	WL [m]	pH	T_{water} [°C]	DO [%]	EC [$mS\ cm^{-1}$]	NO_3^- [$mg\ L^{-1}$]	NH_4^+ [$mg\ L^{-1}$]	TDN [$mg\ L^{-1}$]	NPOC [$mg\ L^{-1}$]
CH	1.5	8.45	12.1	91.40	2.71	0.91	0.12	2.51	37.04
RB	0.2	8.38	10.7	95.80	2.86	0.15	0.23	2.67	40.14
OW	1.5	8.69	5.7	103.50	1.62	0.82	0.28	1.38	16.26

regulated by a three-way stopcock (Discofix, B. Braun SE, Melsungen, Germany) to extract emerging gases (as shown in the top-right picture in Fig. 1). To install the ebullition traps, ambient air was extracted from the funnels and syringes until they were completely filled with water, allowing the board to float with the submerged funnels. A temperature data logger (HOBO Pendant, Model UA-002-08, Onset Computer Corporation, MA, USA) was fixed beneath the board of one trap at each location to record water temperature every 30 min.

To quantify CH_4 ebullition rates during closure period, the gas was extracted from the funnels of the ebullition traps only when there was >1 mL accumulated in the syringe on the collection day. The extracted gas was injected in 20 mL vacuumed glass vials (Agilent Technologies, Inc., Santa Clara, CA, USA), sealed with grey butyl septa (Machery-Nagel GmbH & Co. KG, Düren, Germany) and aluminum crimp caps (Machery-Nagel GmbH & Co. KG, Düren, Germany). The filled vials were stored in a dry and dark compartment at room temperature until analysis, and the storage time was kept as short as possible (from days to a few weeks).

Dry mole fractions of CH_4 and the isotopic signature (δ^{13}C-CH_4 and δ^{13}C-CO_2) of gas samples from the ebullition traps were determined in the lab using a gas and isotope analyzer G2201-i, which uses cavity ring-down spectroscopy (CRDS; a highly sensitive laser absorption technology), connected to a small sample isotope module (SSIM2) (Picarro, Inc., Santa Clara, CA, USA), which enables syringe injection of small gas sample volumes with measurement repetitions. The instrument was calibrated using two certified stable isotope standard gases: one gas cylinder of 2 ppm CH_4 with δ^{13}C-CH_4 of -45 ± 0.5 ‰ VPDB (Vienna Pee Dee Belemnite) and 350 ppm CO_2 with δ^{13}C-CO_2 of -10 ± 0.3 ‰ VPDB, and a second gas cylinder of 10 ppm CH_4 with δ^{13}C-CH_4 of -69 ± 0.5 ‰ VPDB and 1000 ppm CO_2 with δ^{13}C-CO_2 of -20 ± 0.3 ‰ VPDB (Alphagaz, Air Liquide S.A., Paris, France).

Dilution of the gas samples from the ebullition traps was necessary in cases where CH_4 concentrations exceeded the measurement range of the instrument or when the volume of sampled gas was not sufficient for conducting duplicate measurements of each sample. The latter was possible only if the CH_4 concentration in the sample was high enough to conduct dilution and still be in the measurement range of the instrument. For each measurement, a minimum of 15 mL of the (diluted) gas sample was injected into the SSIM2 using a syringe. The measuring protocol was separated into two groups: samples taken in the RB location, and samples taken in the OW and CH locations. This was necessary because, in most cases, the samples from the RB had much higher CH_4

concentrations than those from the other two locations. When a sufficient amount of collected gas (≥12 mL) was available and the concentrations fell within the measurement specification range guaranteed by the Picarro G2201-i instrument (1.8 ppm ≤ CH_4 ≤ 500 ppm, for simultaneous measurement mode of CO_2 and CH_4, high precision or high dynamic range mode), the sample was directly measured. Otherwise, dilution with N_2 gas (6.0, Messer Austria GmbH, Gumpoldskirchen, Austria) was required. Dilutions were performed in 1 L multilayer foil gas bags (Restek Corporation, Bellefonte, PA, USA) using 0.5 L and 1 mL acrylic syringes with PTFE luer lock connectors (Hamilton Company, Reno, NV, USA) and needles (26G Agani, Terumo Corporation, Japan).

2.2.2. Diffusion pathway with floating chambers

To quantify CH_4 diffusion rates at each location, in-situ chamber measurements were carried out using a floating chamber connected to a mobile gas analyzer (Ultra-portable Greenhouse Gas Analyzer (UGGA) for CH_4, CO_2 and H_2O, model 915-0011, Los Gatos Research Inc., Mountain View, CA, USA) on 9 out of the 14 monitoring days. In the remaining weeks, the equipment was not available. The floating chamber was made of transparent PVC in a bird-cage-shape with a diameter of 30 cm. It was supported by an aluminum collar at its base, which was immersed 3 cm into the water. To ensure buoyancy, the collar was girded with a foam tube. During measurements, the chamber was directly connected to the gas analyzer through two 4 mm inner diameter polyurethane tubes (Festo, Esslingen a.N., Germany), one as inlet and the other as outlet, which circulated the air between the closed chamber and the instrument (through-flow system). CH_4 concentrations were registered constantly for 4 min and corrected by the H_2O (water) concentrations. Three replicate chamber measurements were taken at each location on each monitoring day. The water-corrected dry mole fractions of CH_4 were used for further analyses.

2.3. Flux calculations and isotope ratios

Gas concentrations were transformed into fluxes by converting them from ppm to mass per unit volume according to Boguski (2006), and by considering collection time and funnel area. The equation used to estimate CH_4 ebullition fluxes [mg CH_4 m^{-2} d^{-1}] was the following, adapted from Davidson et al. (2018):

$$F_{Eb-CH_4} = \frac{c_{CH_4} \cdot V_{occ} \cdot M_m \cdot p}{R \cdot T_c \cdot A_{fun} \cdot \Delta t} \cdot 10^6 \cdot 1000 \quad (1)$$

where F_{Eb-CH_4} is the ebullition flux of CH_4, and c_{CH_4} is the analyzed CH_4 concentration expressed in ppm. V_{occ} corresponds to the total volume (in L) of occurred gas in the respective syringe from where the gas was collected. A_{fun} is the funnel area (0.0434 m^2) and Δt is the elapsed time in days. M_m is the molar mass of CH_4 (16.04 g mol^{-1}). T_c is the mean air temperature inside the chamber during closure time [K], p is the atmospheric pressure [Pa], and R is the ideal gas constant [kg m^2 s^{-2} mol^{-1} K^{-1}].

Without considering the gas composition in the bubbles captured within the ebullition traps, the bubble flux F_{Bubble} [mL m^{-2} d^{-1}] can be a better proxy, as suggested by DelSontro et al. (2016), to estimate the actual production rate of CH_4 bubbles in sediments and is, therefore, more appropriate for quantifying their control by environmental parameters:

$$F_{Bubble} = \frac{V_{occ}}{A_{fun} \cdot \Delta t} \quad (2)$$

F_{Eb-CH_4} may differ from F_{Bubble} due to the possibility of diffusion (at the gas-water interface) and CH_4 oxidation occurring during ebullition trap closure time (DelSontro et al., 2016), which cannot be excluded, or due to measurement errors during gas collection, dilution or measurement with the gas analyzer.

From the diffusion measurements, the initial 25 % of the floating chamber closure time (death band) was excluded from the linear regression fit of the temporal change of CH_4 concentration inside the chamber. This was done to account for the potential artifacts that may have occurred during chamber closure at deployment, as described by Hoffmann et al. (2017). The diffusion fluxes of CH_4 [mg CH_4 m^{-2} d^{-1}] were calculated with the following equation, adapted from Rochette et al. (1997):

$$F_{Diff-CH_4} = \frac{S}{10^6} \cdot \frac{V_c \cdot M_m \cdot p}{A_c \cdot R \cdot T_c} \cdot 3600 \cdot 24 \cdot 1000 \quad (3)$$

where $F_{Diff-CH_4}$ is the diffusion flux of CH_4, S is the calculated slope of the linear regression of CH_4 concentration change inside the chamber over closure time [ppm(v) s^{-1}], V_c corresponds to the volume of the floating chamber (0.0165 m^3), and A_c is the chamber area where the gas exchange between air and water occurs (0.0707 m^2). Only flux data that had a coefficient of determination $R^2 \geq 0.7$ for linear regression were used. Therefore, about 23 % of all CH_4 diffusion fluxes could not be used due to lack of linearity, especially in the OW location.

The cumulative sums of the diffusion and ebullition rates of CH_4 at each location were calculated for the entire measurement period of 107 days to compare the total amount of diffusion and ebullition.

To estimate the contribution of the major methanogenic type and CH_4 transformation through oxidation, the carbon isotope fractionation factor (α_C, unit-less) between δ^{13}C-CO_2 [‰ VPDB] and δ^{13}C-CH_4 [‰ VPDB] was calculated using the following equation (Whiticar and Faber, 1986):

$$\alpha_C = \frac{(\delta^{13}C - CO_2 + 1000)}{(\delta^{13}C - CH_4 + 1000)} \quad (4)$$

2.4. Water sampling and in-situ measurements

To monitor water quality, in-situ parameters were routinely measured at the water surface of each location, and water samples were collected every 5–10 day throughout the study period (a total of 15 sampling and measurement dates). The in-situ measurements were carried out with a portable multi-parameter meter (WTW, Xylem Analytics Germany Sales GmbH & Co. KG, Weilheim, Germany) connected with water temperature (T_{water}), pH (both Sentix, WTW), electrical conductivity (EC) (TetraCon, WTW), dissolved oxygen (DO) and oxidation-reduction potential (ORP) sensors. For the lab analysis, water was collected from right next to each trap, filtered, and then stored in three 20 mL plastic bottles for each sample. This approach ensured that separate lab analyses could be conducted for each bottle, minimizing the need to thaw the sample multiple times. Filtration of the water samples was done in the field, first with a MN 619 G 1/4 ∅ 125 mm phosphate-free filter paper (Machery & Nagel GmbH & Co. KG, Düren, Germany) due to the high turbidity of the samples at OW and CH, and second, with a 0.45 μm nylon syringe filter to get the dissolved part of the compounds. The plastic bottles with the filtered water samples were transported to the lab in a cooling box containing ice packs. At the end of the sampling day, the samples were stored in a freezer at −20 °C until analysis (Gardolinski et al., 2001; Worsfold et al., 2005).

2.5. Water analysis

The water samples were analyzed in the Geoecology lab of the University of Vienna. Triplicate measurements were taken from each sample in order to analyze the following parameters: nitrate (NO_3^-), nitrite (NO_2^-), ammonium (NH_4^+) and orthophosphate (PO_4^{3-}). Concentrations were determined by colorimetry using a uv-vis spectrometer (Infinite 200 Pro NanoQuant, Tecan Group Ltd., Männedorf, Switzerland) at 540 nm for NO_3^- and NO_2^-, and at 660 and 880 nm for NH_4^+ and PO_4^{3-},

respectively. Sulfate (SO_4^{2-}) was determined by turbidity using the same uv-vis spectrometer at 420 nm. Absorbance values (%) from the uv-vis spectrometer analysis were transformed to concentration units using a standard curve to create a linear regression. The intercept of the regression line was fixed to the average of the blanks, and the R^2 of the linear regression was always higher than 0.98. The procedures used to determine NO_3^- by VCl_3 (Vanadium(III) chloride) reduction, NO_2^-, and NH_4^+, are a modification of the methods described by Miranda et al. (2001) and Kandeler and Gerber (1988), respectively. The procedure used for PO_4^{3-} determination is based on the method described by Murphy and Riley (1962), although modified for analysis using micro-titer plates. The procedure used for SO_4^{2-} determination is based on the method described by U.S.EPA (1999). The dissolved part of the non-purgeable organic carbon (NPOC), inorganic carbon (DIC) and total nitrogen (TDN) were determined from the filtered samples by combustion catalytic oxidation using a TOC-L analyzer (with ASI-L and TNM-L, Shimadzu Scientific Instruments, Inc., Japan).

2.6. Additional data

Biometeorological (Biomet) data were collected from the nearby Eddy Covariance flux tower (EC-tower) (47.769150° N, 16.758482° E), at about 50 m from the RB location (see Fig. 1). Variables such as photosynthetically active photon flux density (PPFD), incoming and outgoing short-wave radiation (SW_{in}, SW_{out}), incoming and outgoing long-wave radiation (LW_{in}, LW_{out}), relative humidity (rH), air temperature (T_{air}), air pressure (PA), water vapour pressure deficit (VPD), precipitation (rain), wind speed (WS), wind direction (WD), soil water content at 5, 10 and 15 cm depth (SWC), soil temperature at 5, 10, and 15 cm depth (T_{soil}), and soil heat flux at 5, 10, and 15 cm depth (SHF) are permanently measured in 1 min time interval. Additionally, T_{air}, rain, rH, SW_{in}, WD, water temperature (T_{water}), and water level (WL) data of Lake Neusiedl were taken from the meteorological station of Hydrographischer Dienst Burgenland (Bgld). This station is located 50 m away from the OW location (47.769996 N, 16.752730 E; see Fig. 1) and has a measurement time interval of 30 min. For each closure period of the ebullition traps and the floating chambers, the mean and the standard deviation (SD) of the environmental variables were calculated to study their potential impact on CH_4 ebullition and diffusion fluxes. In certain cases, variables like temperature were also analyzed for their median, minimum, and maximum values.

2.7. Data processing and statistical analysis

Data processing and statistical analysis were conducted using R (Version 4.2.2, R Core Team (2021)). The R package *data.table* was employed for faster data processing (Dowle and Srinivasan, 2023). For visualization of the results, the R packages *ggplot2*, *ggpubr*, *ggh4x* and *gridExtra* were utilized (Wickham, 2016; Kassambara, 2023a; van den Brand, 2023; Auguie, 2017). Furthermore, the R packages *tidyverse* and *stringi* were applied for data manipulation (Wickham et al., 2019; Gagolewski, 2022).

The non-parametric Kruskal-Wallis test was used to assess whether the medians of the measured fluxes, emission rates and isotopic values of the three location significantly differ. The two-sided Dunn's post-hoc test was applied with the R package *rstatix* (Kassambara, 2023b) to statistically evaluate which locations exhibited significant differences from the others (p-values <0.01, Adjustment Holm). The effect size of the Dunn's test (r) was calculated by dividing the absolute z-value by the square root of the sample size (N). Following Cohen (1988), an r value >0.5 indicates a large effect.

The temperature dependency of the CH_4 ebullition rates at the study site was analyzed using the modified Arrhenius equation, according to Aben et al. (2017). This equation was fitted through non-linear least square regressions (using the R package *nlstools* by Baty et al. (2015)), and all models showed to be statistically significant ($p < 0.01$). The fitted equation includes the modeled CH_4 ebullition rate at 20 °C (E_{20}) and the overall system temperature coefficient (θ_s, dimensionless). A θ_s value of, for example, 1.11, indicates that a 1 °C increase in temperature would lead to an 11 % higher ebullition (Wang et al., 2021a). The non-linear models were compared with the Kling-Gupta Efficiency (KGE, Gupta et al. (2009)) metric to assess the overall agreement with the best-fitting model. An ideal match between simulated and observed values correspond to a KGE value of 1. To facilitate this analysis, the R package *hydroGOF* by Zambrano-Bigiarini (2020) was employed. Additionally, for comparability with other studies, the θ_s values were converted to activation energy (EA) in electron volts (eV) using the conversion equations of Wilkinson et al. (2019). Moreover, for calculating the confidence intervals for the parameters of the Arrhenius models the R package *Rmisc* (Hope, 2022) was used.

Potential relationships between CH_4 ebullition rates or bubble fluxes and environmental parameters (for all locations together, but also separately), were tested using Spearman's rank correlation. This analysis aims to evaluate the strength and direction of monotonic relationships between these variables. Correlations were indicated by the Spearman rank correlation coefficient ρ, with significance determined at p-values <0.01 (Holm's adjustment). For conducting and visualizing the correlation analysis, the R package *ggstatsplot* (Patil, 2021) was used.

3. Results

3.1. Ebullition heterogeneity in space and time

In this study, 311 quality-checked CH_4 ebullition rates were measured along the three locations, from which 88 % had ebullition rates higher than zero. Zero values were included in the ebullitive CH_4 flux estimates because they represent periods during which no ebullition events occurred. Their inclusion ensure that the contribution of the ebullition pathway is not overestimated. Ebullition data were only excluded, when the CH_4 gas measurement with the Picarro instrument did not work well or the ebullition trap broke due to harsh conditions (too strong winds and waves) and needed repairing.

CH_4 ebullition rates showed temporal and spatial variations. They notably increased at the Channel (CH) and Reed belt (RB) locations from March to July 2021 (calendar week from 13 to 27; see Fig. 2B). At the Open water/Lake (OW) location, variations were observed, although no distinct temporal trend was evident. Also, all three locations showed high variance of CH_4 ebullition rates within each location per week. The highest CH_4 ebullition rate (109.20 mg CH_4 m^{-2} d^{-1}) and the strongest increase were, by far, at RB. The median CH_4 ebullition rate at RB is significantly higher than the median of the CH and OW locations (Dunn's post-hoc test, $p < 0.0001$ (Holm's adjustment), effect size $r = 0.7$; see Fig. 2A). The mean CH_4 ebullition rate of the RB location (17.18 ± 28.18 mg CH_4 m^{-2} d^{-1} (± SD)) is >340-fold higher than the mean of the other two locations, 0.05 ± 0.13 and 0.04 ± 0.12 mg CH_4 m^{-2} d^{-1} at the CH and OW locations, respectively.

The temporal variation of the bubble fluxes at the CH and RB locations showed the same increasing trend from March to July 2021 as the CH_4 ebullition rates (compare Fig. S1B to 2B), but unlike the CH_4 ebullition rates, the bubble fluxes at those two locations were nearly in the same range.

3.2. Isotope ratios and fractionation factor of ebullition gas

The stable carbon isotope ratio of CH_4 (δ^{13}C-CH_4) was analyzed in the lab for all the gas samples collected using the ebullition traps. After data quality checking, a total of 274 mean and SD values of δ^{13}C-CH_4 were used for subsequent analysis (see Fig. 3A). The stable carbon isotope ratio of CO_2 (δ^{13}C-CO_2) was also analyzed for all the collected ebullition gas samples but could only be measured for the CH and OW

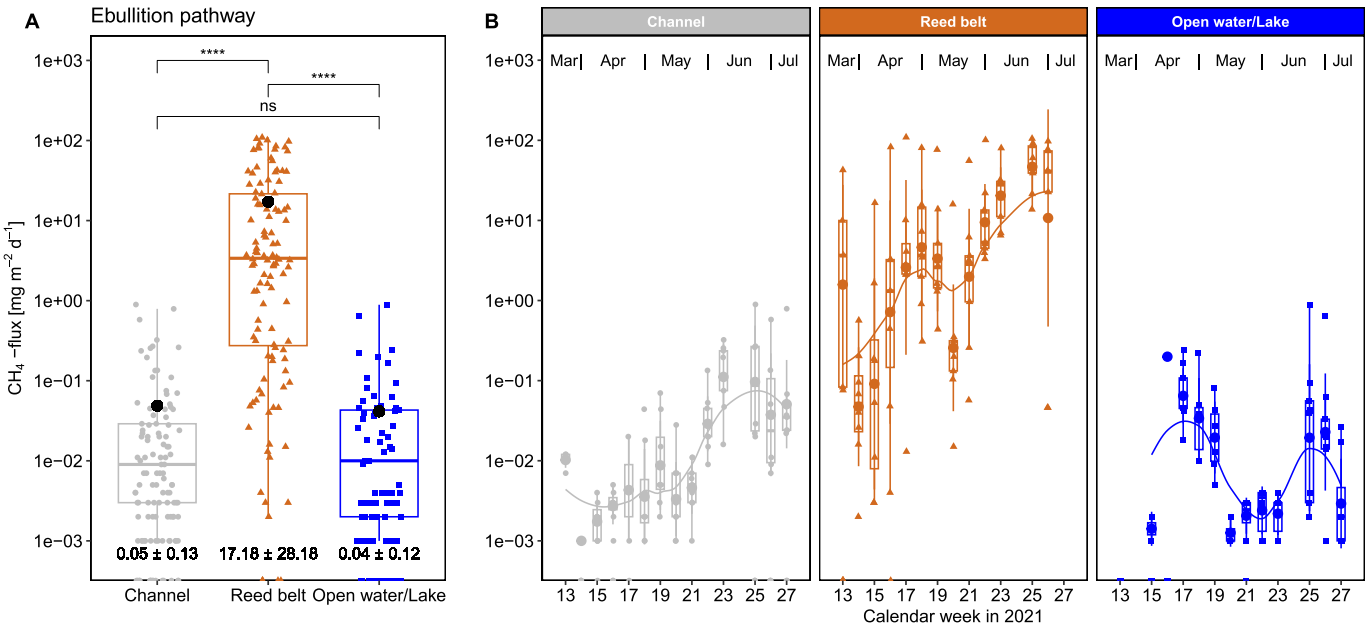

Fig. 2. Methane ebullition rates and their spatial (A) and temporal (B) variability at Lake Neusiedl during the measurement period from March to July 2021 (locations: Channel (CH, grey), Reed belt (RB, brown), and Open water/Lake (OW, blue); black dots (•) showing mean value per location; number under boxplot per location in the left graph is mean ± standard deviation (SD); Dunn's post-hoc test with non-significant (ns, *p*-values >0.05) or very significant (****, p-values <0.0001) differences (Holm's adjustment); the fitted lines show the local polynomial regressions (loess)).

locations. Due to the high CH_4 concentration in the ebullition gas samples from the RB location, high dilution ratios were required (refer to Section 2.2.1). As a result, the diluted gas samples fell below the CO_2 measurement range of the instrument, resulting in (almost) no δ^{13}C-CO_2 values available for RB. Both stable carbon isotope ratios of the measured ebullition gas samples showed some variances within each location per week, and no temporal trend could be observed (see Fig. S2A and B).

The CH location showed a significantly enriched median δ^{13}C-CH_4 compared to the median of the two other locations, RB and OW (Dunn's post-hoc test, $p < 0.0001$ (Holm's adjustment), effect sizes $r = 0.35$ and $r = 0.45$; see Fig. 3A). The median δ^{13}C-CH_4 of the OW was slightly more depleted than the RB but not significantly (ns, *p*-values >0.05). The median δ^{13}C-CO_2 of the CH was significantly more depleted compared to that of the OW ($p < 0.01$, effect size $r = 0.36$; see Fig. 3B).

Combining the two stable carbon isotopes (δ^{13}C-CH_4 and δ^{13}C-CO_2) for estimating the carbon fractionation factor, α_C, the OW location showed a median α_C of 1.05, which is significantly higher than the median α_C of 1.04 of the CH location ($p < 0.0001$, effect size $r = 0.55$; see Fig. 3C). The α_C values of the ebullition pathway ranged from 1.03 to 1.06 at the CH and OW locations, respectively. Following the methanogenic characterization of the measured stable carbon isotope ratios according to Whiticar and Faber (1986) (see Fig. 3D), the measured stable carbon isotope ratios indicate that the dominant methanogenic type for the studied environment, and for our study period, is probably the acetoclastic methanogenesis. This plot also suggest that CH_4 oxidation likely occurred more extensively at the CH location compared to the OW.

3.3. Drivers of methane ebullition

In this study, the drivers of ebullition were addressed in order to better understand the temporal variability (due to temperature dependency) and the spatial heterogeneity (across different locations) in ebullition rates.

A strong temperature dependency of CH_4 ebullition rates was observed at the CH and RB locations, and also with any temperature parameter such as water, air and soil temperature (see Section S3). Meanwhile, at OW, it is likely that factors other than temperature exerted a more pronounced influence on CH_4 ebullition rates. This is indicated by the fact that all non-linear Arrhenius models of the OW location had negative KGE values, which show that these models do not sufficiently fit the data. For the RB, the best non-linear fitting Arrhenius model, with a KGE of 0.35, was with the manually measured mean T_{water} and the CH_4 ebullition rate (see Fig. S3B). In contrast, for the CH, the best fitting model, with a KGE of 0.285, was with T_{water} (HOBO) and the CH_4 ebullition rate (see Fig. S3D). The ebullition rate at 20 °C (E_{20}) at RB, was in all models >400-fold higher than at CH (see Table S1). At the RB location, depending on which temperature was used for the estimation, E_{20} ranged from 12.47 (T_{water}) to 24.82 mg CH_4 m^{-2} d^{-1} (T_{air}). The E_{20} rates of the other two locations, CH and OW, were considerably lower than RB and ranged between 0.03 and 0.06 mg CH_4 m^{-2} d^{-1}, with the highest E_{20} values obtained using T_{air}. The highest θ_s (1.33) and EA (2.21 eV) were found at CH, using T_{water} (HOBO). Whereas the location with the highest ebullition rates (RB), showed lower EA as CH, except for its highest EA (1.47 eV) using T_{soil}.

The Spearman correlation analysis revealed a significant negative correlation between the CH_4 ebullition rate and both the mean WL of the lake ($\rho = -0.68$, $p < 0.01$ (Holm's adjustment)) and the mean NO_3^- concentration at surface water ($\rho = -0.48$, $p < 0.01$; see Fig. S4). In contrast, CH_4 flux via ebullition is positively correlated with other factors: the SD of T_{water} ($\rho = 0.6$, $p < 0.01$), the mean EC of the surface water ($\rho = 0.72$, $p < 0.01$), and the mean NPOC, TDN and SO_4^{2-} concentrations of the surface water ($\rho = 0.65, 0.49, 0.5$, respectively; all $p < 0.01$). The influence of the environmental parameters at the three locations at Lake Neusiedl, characterized by distinct water properties, on the CH_4 ebullition rate is studied in detail by individual correlation analysis (see Figs. S5 to S7).

At the CH location, CH_4 ebullition rates exhibited a significant positive correlation with temperature parameters, such as maximum T_{air} and median T_{water} ($\rho = 0.5, 0.53$, respectively; all $p < 0.01$), as well as with mean PPFD, VPD and DIC concentration of the surface water ($\rho = 0.55, 0.56, 0.43$, respectively; all $p < 0.01$) (see Fig. S5). The ebullition rates of the CH were negatively correlated with the mean WL (Bgld) of

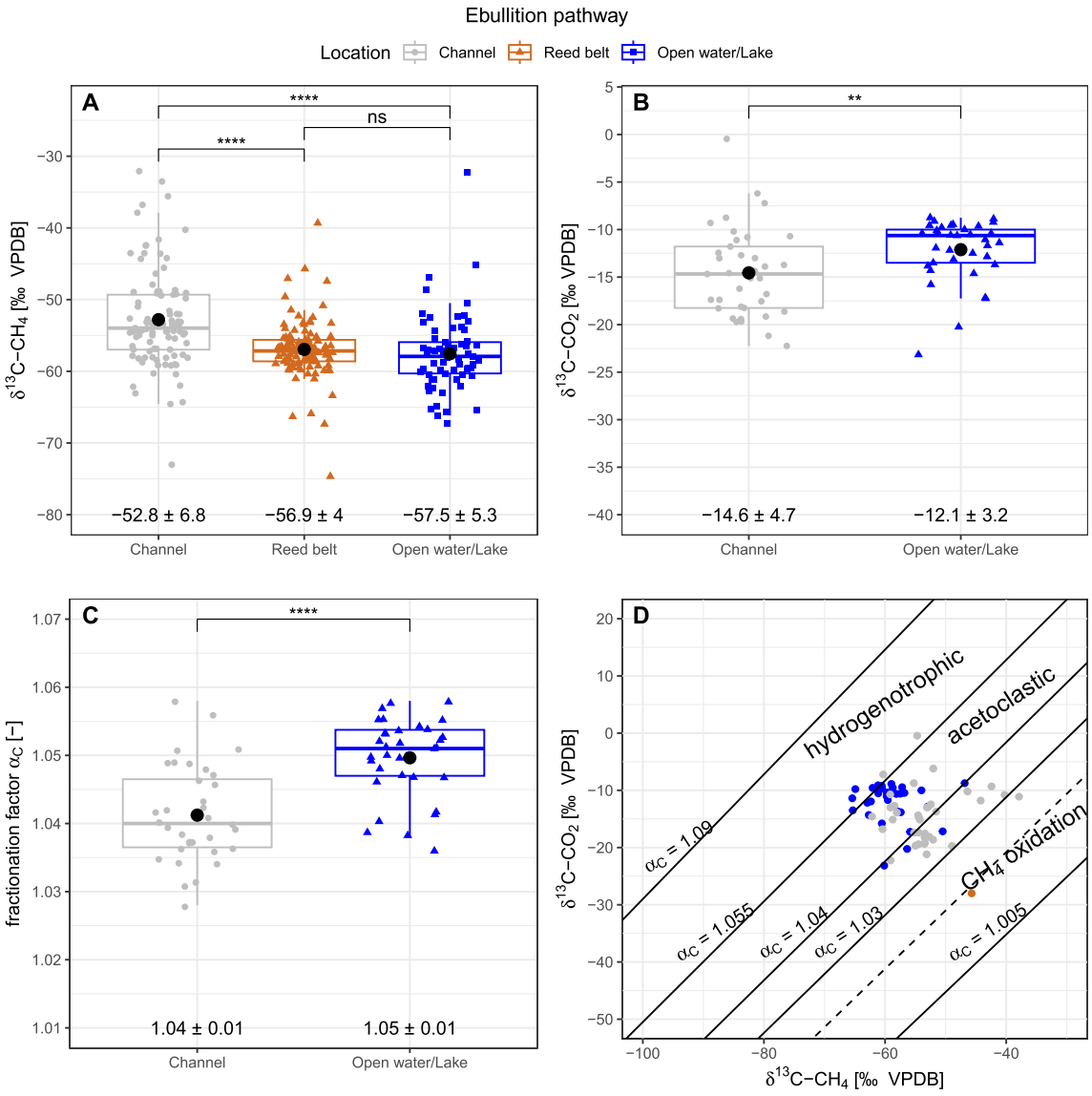

Fig. 3. Stable carbon isotopes δ^{13}C-CH_4 (A) and δ^{13}C-CO_2 (B) and their fractionation factor α_C (C) measured from the ebullition gas samples in the different locations: Channel (CH, grey), Reed belt (RB, brown) and Open water/Lake (OW, blue) at Lake Neusiedl (black dots (•) showing mean value per location; number under boxplot indicating the mean ± standard deviation (SD) per location; Dunn's post-hoc test with non-significant (ns, *p*-values >0.05), significant (**, p-values <0.01) or very significant (****, p-values <0.0001) differences (Holm's adjustment)). D: Methanogenic characterization after Whiticar and Faber (1986) using the measured δ^{13}C-CH_4 - and δ^{13}C-CO_2 - pairs.

the open water area of Lake Neusiedl ($\rho = -0.39$, $p < 0.01$), which is connected to the CH location through a channel.

At the OW location, the CH_4 ebullition rates showed a significant negative correlation with physical environmental parameters, such as, median and maximum PA, mean WD, and mean WL of Lake Neusiedl ($\rho = -0.66, -0.61, -0.54, -0.46$, respectively; all $p < 0.01$) (see Fig. S7). Furthermore, CH_4 ebullition rates also demonstrated a significant positive correlation with the mean DIC concentration of the surface water ($\rho = 0.53$, $p < 0.01$).

In contrast to the other two locations, the RB has the largest number of significantly correlated environmental parameters with the CH_4 ebullition rate (see Fig. S6). The CH_4 ebullition rates at the RB location showed, besides the influence of temperature, a significant negative correlation with mean WL, ORP and maximum PA ($\rho = -0.61, -0.5, -0.44$, respectively; all $p < 0.01$).

Temporal changes in water parameters were observed at CH, RB and OW from late March 2021 to mid-July 2021 and are described in detail in Section S6. From calendar week 27 (mid-July), no water level above the surface was observed at the RB location, therefore, there are no measurements available for this date and the campaign was concluded. Surface T_{water} increased over the measurement period from approx. 9 °C to around 28 °C at CH and OW, and from approx. 10 °C to over 30 °C at RB (see Fig. S10C). In contrast, ORP and WL decreased over the measurement period in all three locations (see Fig. S12A and B).

3.4. Diffusion of methane in space and time

After data quality checking, a total of 62 CH_4-diffusion rates (with $R^2 \geq 0.7$) of the three locations were used for subsequent analysis, accounting for about 77 % of the total measured diffusion rates. The median CH_4 diffusion rate at RB was significantly higher compared to the median at the CH location (Dunn's post-hoc test, $p < 0.01$ (Holm's adjustment), effect size $r = 0.5$; see Fig. 4A). Whereas the other locations were not significantly different from each other's median. Especially at RB and OW, CH_4 diffusion rates varied strongly within each location per week, and no clear temporal trend of the diffusion rates for the entire

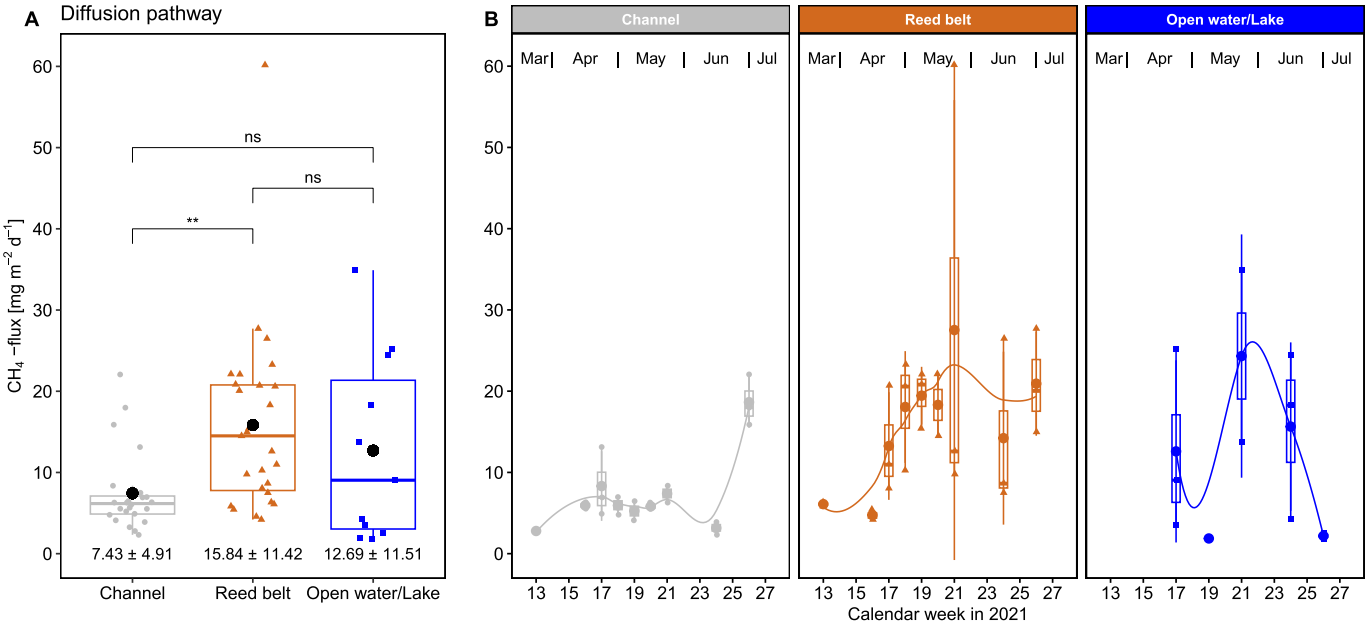

Fig. 4. Methane diffusion rates and their spatial (A) and temporal (B) variability at Lake Neusiedl during the measurement period from March to July 2021 (locations: Channel (CH, grey), Reed belt (RB, brown), and Open water/Lake (OW, blue); black dots (•) showing mean value per location; number under boxplot per location in the left graph is mean ± standard deviation (SD); Dunn's post-hoc test with non-significant (ns, p-values >0.05) or significant (**, p-values <0.01) differences (Holm's adjustment); the fitted lines show the local polynomial regressions (loess)).

study period was evident at any location (see Fig. 4B). Moreover, for the CH_4 diffusion flux, no significant correlation with any available environmental parameter was found.

3.5. Ebullition vs. diffusion pathways

The aim of this part of the study was to explore the dominance or preference of these pathways within the ecosystem on a daily temporal scale and over a certain season (March to July 2021). The ebullition pathway of the CH_4 fluxes showed, at least at CH and RB, an increasing trend from March to July 2021 (see Fig. 2B). In contrast, the diffusion rates displayed no distinct trend, regardless of the location (see Fig. 4B). Independent of the location, the CH_4 ebullition rates had larger variance within each location per week than the CH_4 diffusion rates.

The median CH_4 diffusion rates were significantly higher than the median CH_4 ebullition rates in all three locations at Lake Neusiedl, especially at CH and OW (Dunn's post-hoc test, $p < 0.0001$ (Holm's adjustment), effect size $r = 0.66$ and 0.55; see Fig. 5). Nevertheless, at the RB location, the mean CH_4 ebullition rate (17.18 mg CH_4 m^{-2} d^{-1}) was higher than the mean CH_4 diffusion rate (15.84 mg CH_4 m^{-2} d^{-1}). For both pathways, the RB location showed the highest CH_4 fluxes and the widest range (see Table S2).

For a better comparison between the two pathways, ebullition and diffusion, the cumulative sums of CH_4 fluxes were calculated for each ebullition trap or floating chamber at every location. This calculation spanned the entire study period. At CH and OW, the median cumulative CH_4 diffusion rates were significantly higher than the cumulative CH_4 ebullition rates ($p < 0.05$, effect size $r = 0.80$), whereas at RB, no

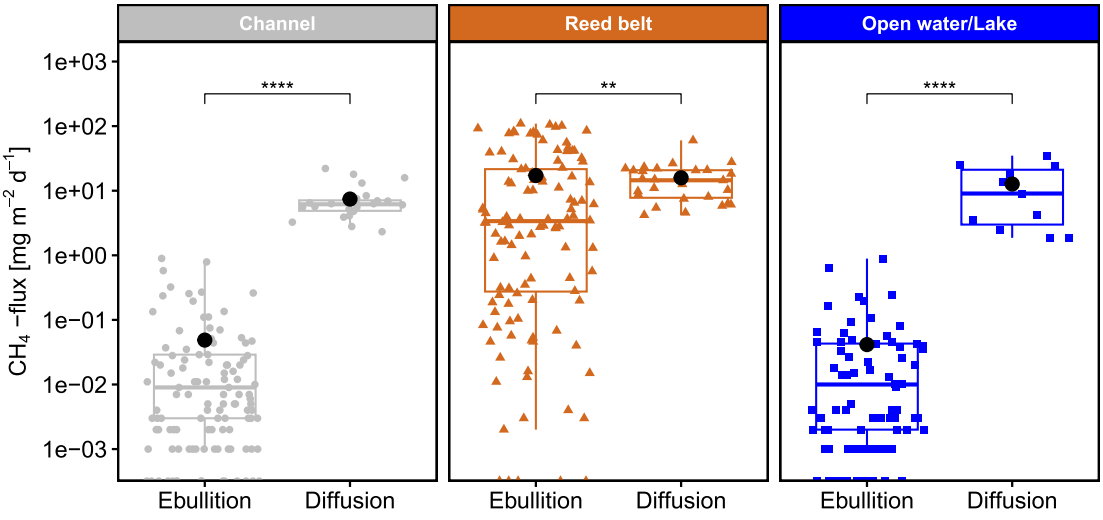

Fig. 5. Methane ebullition and diffusion rates and their spatial variability at Lake Neusiedl during the measurement period from March to July 2021 (locations: Channel (CH, grey), Reed belt (RB, brown), and Open water/Lake (OW, blue); black dots (•) showing mean value per location; Dunn's post-hoc test with significant (**, p-values <0.01) or very significant (****, p-values <0.0001) differences (Holm's adjustment)).

significant difference was observed in the cumulative CH_4 rates between the ebullition and diffusion pathways (see Fig. 6A). The median cumulative CH_4 diffusion rates were not significantly different between the locations, neither the cumulative ebullition rates between the CH and OW locations. Nevertheless, the cumulative CH_4 ebullition rates at RB were significantly higher compared to the CH and OW locations ($p < 0.001$, effect size $r = 0.83$ and 0.87, respectively). For both pathways, the highest mean cumulative CH_4 fluxes were found at RB, and, as a result, also the highest sum of the cumulative CH_4 ebullition and diffusion rates (see Fig. 6B). The mean (±SD) share of the ebullition pathway on the total cumulative CH_4 emissions was 47.8 ± 17.0 % for the RB location, whereas for the CH and OW locations, it was 1.2 ± 1.9 % and 0.7 ± 0.7 %, respectively.

By far, the highest cumulative sum of the bubble fluxes was found at OW (see Fig. 6C), and not at RB location like for the cumulative CH_4 ebullition rates. The median cumulative bubble flux at the OW location was significantly higher compared to CH ($p < 0.001$, effect size $r = 0.95$) and to RB ($p < 0.01$, effect size $r = 0.66$). Meanwhile, the lowest mean cumulative sum of bubble fluxes was found at CH.

4. Discussion

4.1. Ebullition heterogeneity in space and time

This study explored the occurrences and CH_4 ebullition rates across three representative locations of Lake Neusiedl, continuously from late March to mid-July 2021. The location within the reed belt of Lake Neusiedl (RB) exhibited, by far, the highest CH_4 ebullition rates over the entire measurement period. One explanation for the elevated CH_4 ebullition rates at RB in comparison to the other two locations, may be the greater availability of organic matter, including both fresh and old reed biomass, along with higher NPOC concentrations in the RB area. This can be assumed by the fact that RB, in contrast to the other two locations, shows a significant positive correlation between NPOC and ebullition rate (see Fig. S6 in contrast to Figs. S5 and S7). Another contributing factor might be the lower water levels at the RB site, leading to enhanced methanogenesis within the sediments due to elevated sediment temperatures compared to the other locations. This relationship can be confirmed by a significant negative correlation between water level and T_{soil} at the RB location (see Fig. S6).

The increasing trend in CH_4 emission rates, particularly at the RB site (but also at the CH site) from March to July 2021 (see Fig. 2B), can be attributed to the seasonal pattern of influencing factors such as temperature and is therefore discussed in more detail in Section 4.3.

Although the mean and median CH_4 ebullition rates at CH and OW were not significantly different from each other, their temporal pattern over the measurement period varied. This disparity could be potentially attributed to distinct factors driving the release of bubbles, and perhaps with lesser influence, due to the different CH_4 production rates. This is shown by the fact that in OW the ebullition rate is influenced more by physical parameters (wind direction and air pressure), whereas in CH the temperature plays a major role (compare Fig. S7 with S5). The differences between the locations could also be explained by considering that the produced CH_4 has been oxidized more strongly. Although ebullition is characterized for rapid release from the sediments to the atmosphere, allowing little to no reaction within the water column to occur, it cannot be completely ruled out. In addition, it should be noted that both CH and OW locations have consistently higher water levels than RB, and thus, a larger water column for interaction opportunities. Nevertheless, if CH_4 oxidation occurs, it is more likely to happen in the

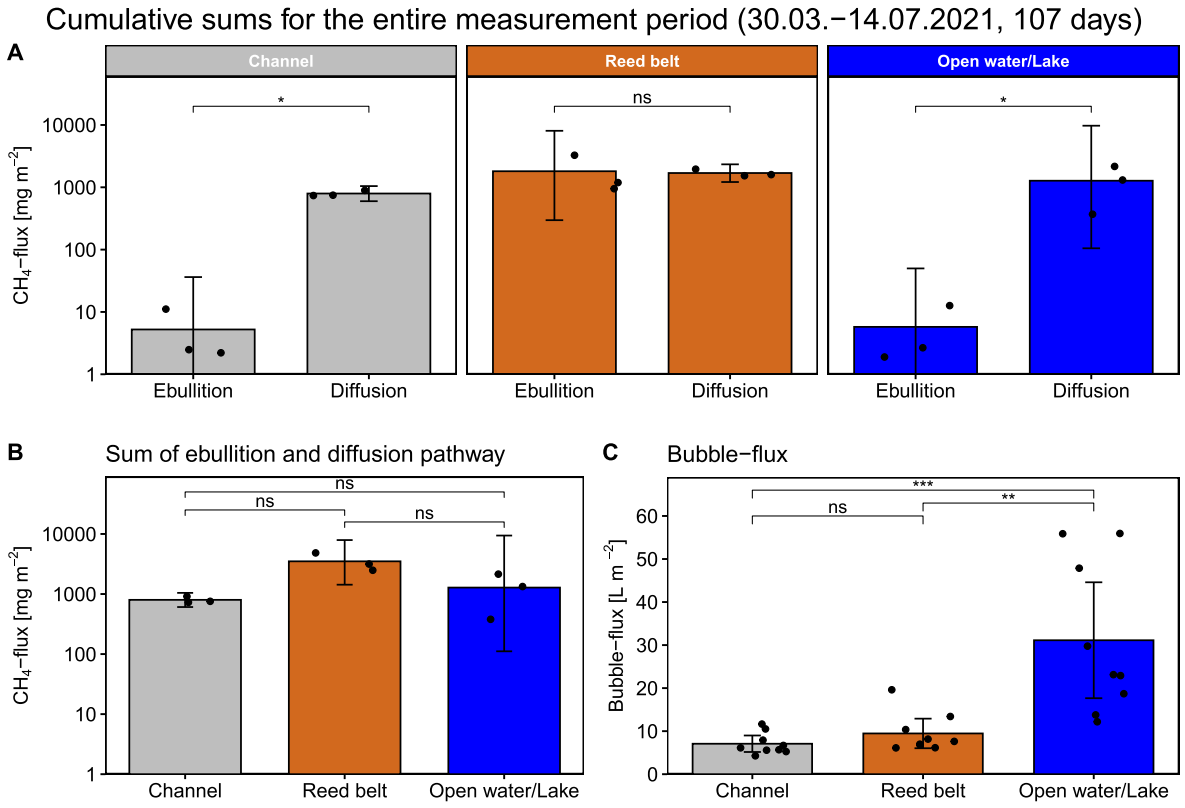

Fig. 6. Cumulative sums of CH_4 ebullition and diffusion rates (A), total CH_4 emission rates (B), and bubble fluxes (C) for the entire measurement period of 107 days, separated by the three locations: Channel (CH, grey), Reed belt (RB, brown), and Open water/Lake (OW, blue). Black dots (•) showing the replicated measurements per location; colored bar indicates the mean value of the replicates per location; error bar presents the 95% confidence interval (CI) of the replicates per location; Wilcoxon signed-rank test with non-significant (ns, $p > 0.05$), significant (*, p-values <0.05), (**, p-values <0.01) or (***, $p < 0.001$) differences (Holm's adjustment).

upper sediments rather than in the water column, if it occurs at all. We assumed this because in our study we did not find any correlation between the ebullition rate and the DO values in the water column.

Whereas the CH_4 ebullition rates showed strong differences between RB and the other two locations, the mean bubble flux showed no significant differences among any of the locations. This might be due to the reduction of CH_4 concentration in the trapped bubbles during the closure time due to diffusion (at the gas-water interface) or CH_4 oxidation. If this factor indeed had an impact, its magnitude would likely differ between the locations, resulting in different rates. Nonetheless, it is more likely that varying levels of CH_4 production in the sediments between the three locations explain the strong differences in ebullition rates. The OW location, which showed the highest bubble fluxes, experiences the strongest wind and wave influences, potentially triggering more frequent bubble release with distinct volumes and possibly lower concentrations compared to the other locations. This assumption can be confirmed by the fact that in OW, the bubble flux shows a significant positive correlation with the wind speed in contrast to the ebullition rate (see Fig. S7). Perhaps these wind and wave conditions also explain why the OW location showed an almost 3-fold higher mean and 5-fold higher maximum bubble flux compared to Canadian lakes (DelSontro et al., 2016), which share similar shallow conditions to Lake Neusiedl, but may not experience such strong winds and waves. However, the extent of this effect requires further investigation.

Soja et al. (2014) estimated ebullitive CH_4 emissions at Lake Neusiedl using the same measurements they utilized for estimating CH_4 diffusion flux on six distinct days between 2011 and 2012. They did not employ a separate methodology such as ebullition traps. The authors used the CH_4 concentration leaps (if they occurred) during the 30-min closure time of the floating chambers as a basis to calculate the ebullitive flux. Using this method, Soja et al. (2014) observed ebullition only in 40 % of the chamber measurements. In contrast, our study conducted at Lake Neusiedl involves continuous measurements of ebullition rates, documenting ebullition occurrences in 88 % of all observations. This suggests that measurements with ebullition traps offers a more comprehensive coverage of the spatial and temporal heterogeneity of ebullition compared to non-separate measurements using floating chambers. Furthermore, Soja et al. (2014) do not provide average ebullition rates, though most of their reported ebullition rates seem to be higher than our values.

Among the very few studies related to ebullition in subsaline lakes, Aguirrezabala-Campano et al. (2019) did not detected ebullition in subsaline ponds in Spain during a total of 40 h of continuous CH_4 measurement. The reason for this is not entirely clear, but one possibility could be that the short measurement period did not capture the sporadic release of ebullition bubbles. To avoid this possibility, we used longer closure time of ebullition traps (5–10 days) in our study. A study by Wang et al. (2021b) with potentially two subsaline lake sites (thermokarst lakes with conductivity values >1 mS cm^{-1}) found a negative correlation of the ebullition rate with salinity and therefore the lake site with lower conductivity showed the highest mean ebullition rate (27 mg CH_4 m^{-2} d^{-1}). In our study, however, it was the other way around, we found a positive correlation between ebullition rate and conductivity (see Fig. S4), because the location with the highest conductivity in the water (RB) showed the highest ebullition rates. At Lake Neusiedl, the rising conductivity values in the water of all three locations can be probably explained by the increasing concentration of salt due to the decline in water levels from March to July 2021 and the general differences of the water levels between the locations (see Figs. S10B and S12B). The increasing concentration of salt may occur less in sediments than in the water column and therefore might not significantly contribute to the different CH_4 production rates between locations. Furthermore, Poffenbarger et al. (2011) confirmed that CH_4 emissions (from tidal marshes) decrease with increasing salinity, but only polyhaline systems (salinity >18 ‰) showed significantly lower CH_4 emissions. However, oligohaline marshes (salinity 0.5–5 ‰), which are comparable to subsaline lakes due to their salinity, have the most variable and significantly higher CH_4 emissions than other saline or freshwater systems (Poffenbarger et al., 2011). The high variability of CH_4 emissions from a subsaline lake can be confirmed with this study (see Table S2).

Because there is hardly any published CH_4 ebullition study of subsaline lakes, a comparison with other (shallow) lakes is made. On average, CH and OW had very low CH_4 ebullition rates compared to RB (see Table S2), to the global mean ebullition rate of freshwater lakes (40.1 mg CH_4 m^{-2} d^{-1}; Zheng et al. (2022)), and to other related studies (Aben et al., 2017; Bogard et al., 2014; DelSontro et al., 2016; Bastviken et al., 2008). For example, the mean ebullition rates observed in OW or CH are 100-fold smaller than the mean ebullition rate from the small shallow lake Hummingbird, which is the lake with the lowest mean ebullition rate in the study of Bastviken et al. (2008). In contrast, the mean CH_4 ebullition rate at RB in our study is around 1.8-fold higher than the average ebullition flux recorded in the small shallow Lake Jacques during the dry summer of 2012, as reported by Bartosiewicz et al. (2015). Whereas the mean ebullition rate at RB is almost in the same range as the average ebullition rate of three Canadian lakes (17.6 mg CH_4 m^{-2} d^{-1}), where ebullition only occurred in water levels <3 m (DelSontro et al., 2016). A possible explanation for this discrepancy could be that the salinity and sulfate concentration at Lake Neusiedl might have reduced or somewhat suppressed CH_4 production, consequently leading to lower CH_4 emission rates in comparison to Lake Hummingbird, the global mean ebullition rate of Zheng et al. (2022), and other studies. Although most of these studies are from northern and small shallow lakes, which have different climatic and lake characteristics compared to our studied temperate, large, shallow and subsaline Lake Neusiedl, the RB location still has similar ebullition rates to some lakes. Presumably, the lower ebullition rate, especially in the OW location, can be better explained by the lower availability of substrate for CH_4 production.

In subsaline lakes, such as Lake Neusiedl, where salinities of 10–15 ‰ (Wang et al., 2017) are not reached, sulfate reduction and CH_4 production are processes that most likely occur at the same time and next to each other, allowing sulfate-reducing bacteria and methanogens to coexist and compete (Rosentreter et al., 2021). The ability of sulfate-reducing bacteria to outcompete methanogenic bacteria is well known. Lovley and Klug (1983) reported this process to occur even at freshwater sulfate concentrations. More recently, Kleint et al. (2021) reported CH_4 to be consumed via sulfate in sulfate–methane transition zones that have been observed for a few specific freshwater environments only. We did not examine these transition zones in the spatial resolution required to clearly detect them. Nevertheless, it appears reasonable that a gradient in the redoxcline found in a freshwater lake (Lake Willersinnweiher) by Kleint et al. (2021), can be also found in a subsaline environment such as Lake Neusiedl. Although, the δ^{13}C-CH_4 values that we encountered are more depleted than the ones determined in Lake Willersinnweiher around the redoxcline.

Ebullition rates are rarely determined continuously, they are rather estimated as a side product of diffusion measurements using floating chambers on specific sampling days during daytime (Wang et al., 2021b; Linkhorst et al., 2020; Soja et al., 2014; Käki et al., 2001). These short-term ebullition measurements probably miss most ebullition events, leading to an underestimation of the ebullition pathway (Bastviken et al., 2011; Wik et al., 2016). Some studies stir the sediments to artificially release the bubbles (Thottathil and Prairie, 2021; Schenk et al., 2021; Männistö et al., 2019), which can be used to estimate the original CH_4 concentration or the isotopic signature of the bubbles within the sediments (DelSontro et al., 2016). However, we needed an approach that could capture the temporal patterns of ebullition with the naturally released bubble size. Therefore, we desist from manually triggering ebullition events (unlike Thottathil and Prairie (2021)), as our aim was

to investigate the natural ebullition occurrences and their underlying drivers, while preserving the integrity of the sediment surface by avoiding stirring. Furthermore, we chose to use bubble traps with longer closing times (5–10 days as e.g., in McClure et al. (2020); Aben et al. (2017)), which proved to be optimal for our study site, ensuring the accumulation of the minimum gas volume for extraction at all locations. It is important to note that this approach holds its own drawbacks, including plausible errors such as the underestimation of ebullition rates due to potential exchange between the trapped CH_4 and the underlying water column or the possible oxidation of the trapped CH_4 (DelSontro et al., 2016), or potential diffusion from the syringe to the atmosphere through the plastic and the stopcock during the closure period of the ebullition traps.

4.2. Isotope ratios and fractionation factors of ebullition gas

The measured δ^{13}C-CH_4 values from this study confirmed the biogenic (also called 'bacterial' or 'microbial') origin of CH_4 at Lake Neusiedl, according to Whiticar (1999). Both, the δ^{13}C-CH_4 and α_C values obtained in this study can be isotopically classified as indicative of CH_4 originating from freshwater sediments, in line with the classification provided by Whiticar and Faber (1986), and discarding a marine origin. Only a few α_C values were lower than 1.04, probably due to CH_4 oxidation. While Lake Neusiedl is not a marine ecosystem, it should be noted that due to its high salinity (2.1–5.2 g L^{-1}, transformed from EC values with the regional constant correction of Boros et al. (2014) due to the special salt composition, see Fig. S10B), the lake cannot be longer defined as a freshwater system (salinity <1 g L^{-1}), but is rather classified as a subsaline lake according to Hammer (1986). Furthermore, both the water column of Lake Neusiedl and the pore water in the upper sediments have high sulfate concentrations, ranging from 250 to 1250 mg SO_4^{2-} L^{-1} (see Fig. S9A). These levels are typically found in brackish waters or even seawater, which would likely suppress CH_4 production.

Ebullition is recognized for lacking C fractionation, opposed to other processes such as diffusion or CH_4 oxidation. Therefore, the isotopic signature of the ebullition gases could be used as an indicator of the CH_4 source in the sediments. For Lake Neusiedl, this estimate would average -55.6 ± 5.9 ‰ VPDB δ^{13}C-CH_4.

The α_C values derived from this study suggest the prevalence of the acetoclastic methanogenesis type at CH and OW according to Whiticar and Faber (1986) and Thottathil and Prairie (2021). Unfortunately, we are unable to provide a statement regarding the α_C values at RB, as the δ^{13}C-CO_2 measurements were not feasible at that location. Nevertheless, considering that the δ^{13}C-CH_4 values at RB are in the same range as at OW, it is likely that they share the same predominant methanogenesis type. Also the fact that most organic material is found within the reed belt, which serves as main substrate for the dominant acetoclastic CH_4 production, could explain, among other reasons, the significantly higher CH_4 ebullition rates at the RB location in comparison to the other locations.

Furthermore, our study did not show a shift in methanogenic types with depth from acetoclastic (shallow water) to hydrogenotrophic methanogenesis (deep water) as in Wik et al. (2020); Thottathil and Prairie (2021). One reason could be that Lake Neusiedl is generally too shallow and therefore has no deep water zones. A second reason could be that the root exudates of the reed influence the entire lake, which is why acetoclastic methanogenesis dominates. A third reason could be that Lake Neusiedl and its microbial community are different from the studies of the northern lakes by Wik et al. (2020); Thottathil and Prairie (2021) due to the different climatic (and environmental) conditions.

At Lake Neusiedl, the acetoclastic methanogenesis was likely dominant throughout the entire study period, because δ^{13}C-CH_4 and δ^{13}C-CO_2 showed minor temporal variability (see Fig. S2A and B). This result is in contrast to the temporal pattern of the isotopic signature found in the study of Thottathil and Prairie (2021), which included a seasonal shift from hydrogenotrophic to acetoclastic methanogenesis over the season due to the change in substrate supply. The absence of a temporal pattern of the isotopic signature in our study could be due to the fact that the seasonal shift of methanogenesis types has not yet occurred, as there may not have been any relevant change in substrate availability. However, our study at Lake Neusiedl already showed a dominance of acetoclastic methanogenesis in spring and early summer, which is why a shift from hydrogenotrophic to acetoclastic cannot actually occur anymore. Nevertheless, acetoclastic methanogenesis seems to be more dominant in shallow than deep waters (Wik et al., 2020; Thottathil and Prairie, 2021), which we could confirm with this study for at least two locations in the shallow Lake Neusiedl.

Although the two locations, CH and OW, showed both a dominance in the diffusion compared to ebullition pathway (see Fig. 5), they showed a significant difference in their median δ^{13}C-CH_4 values (see Fig. 3A). This could be explained by the fact that in diffusion dominated systems, the variations in the extent of the CH_4 oxidation, besides the methanogenesis types, determine the isotopic signature of the emitted CH_4 (Happell et al., 1994). Whereas in ebullition dominated systems, variations in CH_4 production mechanisms mainly control $\delta^{13}C$-values of emitted CH_4 (Happell et al., 1994).

On average, CH exhibits more enriched δ^{13}C-CH_4 values compared to the other two locations. This could be attributed to higher CH_4 oxidation rates at CH, which tend to favor the lighter stable carbon isotope (^{12}C), resulting in an enrichment in δ^{13}C-CH_4 at this site in comparison to the other locations. δ^{13}C-CO_2 values were notably more depleted at CH (mean δ^{13}C-CO_2 of -14.6 ± 4.7 ‰ VPDB) compared to OW (see Fig. 3B). This observation suggests that CH_4 oxidation likely occurred more intensively at CH compared to OW. Nevertheless, CH_4 oxidation at CH seems to be noticeably lower than, for instance, in a tropical lake that showed δ^{13}C-CO_2 values <−35 ‰ VPDB (Miller et al., 2022). At OW, CH_4 oxidation probably played a minor role, since the δ^{13}C-CO_2 values only showed slight depletion compared to atmospheric values.

The reed plant *Phragmites australis* is known to enhance aeration in certain parts of the rhizosphere through aerenchymatic oxygen (O_2) transport (Armstrong and Armstrong, 1990), facilitating CH_4 oxidation in the sediments. Moreover, in wetlands, the acetate production is commonly higher within the rhizosphere of vascular plants such as *P. australis* because of organic matter decay and root exudates, which favors the acetoclastic type of methanogenesis (Ström et al., 2003, 2005). The reed not only dominates the vegetation cover in the RB location but also surrounds the channels at the CH location. Therefore, our results corroborate this notion of Ström et al. (2003, 2005), as α_C in the CH location is lower than in the OW location (see Fig. 3C and D), indicating a higher contribution of acetoclastic methanogenesis. However, a few α_C values from the RB location are even lower, beyond this range, indicating the occurrence of CH_4 oxidation.

4.3. Drivers of ebullition

The identified drivers of CH_4 ebullition fluxes differ among studies. Some studies found a temperature dependency of CH_4 ebullition rates, resulting indeed in seasonal patterns (Aben et al., 2017; Wang et al., 2021a; Thottathil and Prairie, 2021). The CH_4 ebullition rate may even rise by 6–20 % per 1 °C global temperature increase (if organic matter is not limited), thereby contributing to further global warming (Aben et al., 2017). Whereas Wang et al. (2021b) found no clear seasonal pattern of CH_4 ebullition rates related to temperature changes at thermokarst lakes on the Tibetan Plateau. In our study, we can confirm a seasonal pattern of ebullition (increasing trend from March to July 2021) at two of three sites on Lake Neusiedl, showing that even within a lake (and not only between lakes) the drivers of ebullition can be different.

According to DelSontro et al. (2016), this temperature dependency of ebullition is regulated by the ecosystem's trophic status (in their case,

determined by total phosphorus) and weakens in oligotrophic lakes due to limitations in organic substrate availability. In addition, the study states that a strong positive interaction between phosphorus and temperature controls the predominant emission pathway where ebullition is disproportionately boosted. As CH_4 production is a function of temperature and Lake Neusiedl is eutrophic, we anticipated that ebullition rates would increase in all locations due to the persistent increase in water temperature, added to the fact of shallow water levels. This phenomenon was observed at RB and CH but not at OW. In the RB and CH locations, we could observe a temperature dependency of the ebullition rates, consistent with the findings of Aben et al. (2017), although they excluded saline and brackish waters in their study. However, our highest modeled E_{20} value at RB (24.82 mg CH_4 m^{-2} d^{-1}), which represents CH_4 ebullition at 20 °C, was 10-times lower than the E_{20} values for the most comparable ecosystem (temperate ponds) in the study by Aben et al. (2017). These substantial differences could be attributed to variations in ecosystem types, nutrient status, organic matter availability, salinity, pH, or differences in the measurement intervals of the ebullition traps (24 h vs. 1 week) and associated effects (as mentioned in Section 4.1). Nevertheless, the overall system temperature coefficient, θ_s, at RB falls within the same range (1.11–1.22) as that of temperate ponds studied by Aben et al. (2017), with only the values at CH being higher (1.22–1.33). Especially the range of EA from the CH location (1.47–2.21) is higher than the mean ecosystem-level EA estimate of 0.96 eV in Yvon-Durocher et al. (2014) but still within the upper range of ecosystem-level EA estimates (<2.5 eV, Yvon-Durocher et al. (2014)) as well as in the range of ponds (1.75 eV, DelSontro et al. (2016)) and temperate shallow lakes (1.85 eV, Schmiedeskamp et al. (2021)). Some differences could also result from differences in the used equations for conversion of θ_s to EA from Wilkinson et al. (2019). Nevertheless, both, the EA and the θ_s, indicated a high temperature-sensitivity of the ebullition pathway and its higher contribution with increasing temperature at the CH and RB locations at the shallow subsaline Lake Neusiedl. However, the values vary greatly depending on whether one takes soil-, water- or air-temperature (see Table S1), which is why comparability may only be possible with the same temperature parameter.

As outlined by DelSontro et al. (2016), the processes influencing CH_4 emissions are more complex than originally thought. CH_4 ebullition rates not only depend on temperature but are rather regulated by an interaction between trophic status (e.g., total phosphorus) and temperature. In our study at Lake Neusiedl, we did not identify a correlation between the CH_4 ebullition rate and PO_4^{3-} concentrations in the surface water. However, we did observe a positive and significant correlation of the ebullition rate with the TDN concentrations in the surface water (see Fig. S4). In contrast, the nitrate concentration correlated negatively with the ebullition rate. This negative relationship, as discussed in Flury et al. (2010), can be explained by the possible coupling between CH_4 oxidation in the water column with denitrification. Similar to the effect of temperature increase, enhanced nitrogen availability (through e.g., deposition) can also stimulate methanogenesis through higher production of organic matter, consequently leading to an increase of CH_4 emissions (Flury et al., 2010).

In their study, Bogard et al. (2014) linked acetoclastic CH_4 production in the oxic water column to algal dynamics, indicated by chlorophyll *a* concentration in water. Particularly within the reed belt of Lake Neusiedl (CH and RB locations), along the reed stands, we observed some algal growth during the study period. On 29 March 2021, the average chlorophyll *a* concentration was <1 μg L^{-1} in the RB and CH locations, and about 17 μg L^{-1} in the OW location. By 28 June 2021, the chlorophyll *a* concentration in the water had increased to about 40 μg L^{-1} at OW, 56 μg L^{-1} at RB, and 80 μg L^{-1} at CH. OW exhibited the highest increase in chlorophyll *a*, even though it did not have the highest CH_4 rates at Lake Neusiedl, unlike RB. Unfortunately, we have not continuously measured chlorophyll *a* in the water throughout the entire study period. Thus, the statement of Bogard et al. (2014) cannot be confirmed at Lake Neusiedl with the current knowledge.

In northern temperate lakes, higher CH_4 ebullition rates were connected with an enrichment in $\delta^{13}C$-CH_4 values by supporting the prevalence of acetoclastic methanogenesis (Thottathil and Prairie, 2021). In contrast to Thottathil and Prairie (2021), we found no significant correlation between the ebullition rates and the $\delta^{13}C$-CH_4 values, despite the dominance of acetoclastic methanogenesis. This discrepancy could be due to the different lake characteristics and the occurrence of *P. australis*.

4.4. Diffusion of methane in space and time

CH_4 diffusion is a function of the gradient of CH_4 concentrations at the water-air interface. This gradient can be influenced by various factors, including wind (and waves), mixing of the water column and the solubility of CH_4 gas in the water, with the latter being influenced by temperature, salinity and pressure. Nevertheless, the primary influencing factor for diffusion flux is methanogenesis and its production rates.

In this study, the diffusion pathway was primarily measured for the purpose of comparison with the ebullition pathway. In all three locations at Lake Neusiedl, the water temperature increased over time (see Fig. S10C), which should have also increased the solubility of CH_4 gas in water. The salinity of the surface water, which can be estimated with the EC value (see Fig. S10B), increased slowly over time at the CH and OW locations, but very strongly at the RB location due to the more pronounced decrease of the water level. This decrease in water level would likely have decreased the solubility of CH_4 gas in water. Pressure fluctuations at all locations occurred during the study period, which could have also altered the solubility of CH_4 gas in water, but it would likely influence all three locations in a similar matter. Moreover, both the maximum and highest mean CH_4 diffusion rates were observed at the RB location. This could be attributed to several factors, including the higher salinity of the surface water, lower water levels, and the influence of wind on the water pools inside the reed belt.

In the OW location, the mean CH_4 diffusion rate was approximately 40 % higher than at CH. These two locations had similar water levels, but the DO content in the water was higher at the OW location most of the time (see Fig. S11B). Taking into account the strong wind that exists at Lake Neusiedl, particularly in open water areas not protected by the reed, wind might be regarded as a crucial physical driver for diffusion emissions at OW due to its role in water mixing and the transport of new air parcels.

At Lake Neusiedl, Soja et al. (2014) conducted measurements of diffusive CH_4 fluxes during 2011/2012 with six-month intervals and employed long closure periods for the floating chambers (30 min). The authors found that high CH_4 diffusion rates were observed at water channels within the reed belt only in early spring (April 2012), which may be attributed to delayed ice melt that resulted in the winter-delayed methane diffusion peak. Otherwise, the water channels exhibited CH_4 fluxes approximately two-thirds lower than the rest of the reed belt (Soja et al., 2014). In contrast, our study demonstrates that there were no high diffusion rates observed during spring 2021, since there was no ice cover present at any location. However, the CH_4 diffusion rates we obtained in the CH location were, on average, up to half lower than those in the other two locations (RB and OW). This discrepancy could potentially be attributed to the more wind- and wave-protected nature of the CH location. In 2011/2012, the diffusion rates at Lake Neusiedl ranged from 2 to 50 mg CH_4 m^{-2} d^{-1} (Soja et al., 2014), which falls within the same range as our observations. However, it is worth noticing that in our case, the diffusion rate exceeded the 35 mg CH_4 m^{-2} d^{-1} only once.

The mean CH_4 diffusion rate at OW (12.7 mg CH_4 m^{-2} d^{-1}) falls within the same range as the global mean diffusion flux from freshwater lakes (Zheng et al., 2022) and the average pelagic diffusive flux from lake Cromwell (Bogard et al., 2014). Depending on the amount of

precipitation in summer, a small shallow lake (Bartosiewicz et al., 2015) showed a slightly higher mean diffusion flux (dry summer) than our study or a lower flux (rainy summer) than two locations in our study. Whereas the average diffusion flux of three Canadian lakes (DelSontro et al., 2016) is more than twice as large as the highest mean diffusion flux (15.8 mg CH_4 m^{-2} d^{-1}, RB location) in our study. These differences could be explained by the different measurement periods between the respective studies (March–July vs. May-Oct) or to the differences in lake characteristics.

In comparison to subsaline ponds in Spain (ranging from 0.12 to 0.98 mg CH_4 m^{-2} d^{-1}; Aguirrezabala-Campano et al. (2019)), the diffusive CH_4 rates of our study were clearly higher. However, these ponds have significantly higher concentrations of sulfate in the water (>1.2 g L^{-1}) than the subsaline Lake Neusiedl, which likely resulted in lower CH_4 production.

4.5. Ebullition vs. diffusion pathway

The ebullition pathway is rarely estimated because of the sporadic nature of ebullition episodes and their significant spatial heterogeneity. This makes determining ebullition challenging, potentially leading to an underestimation of CH_4 emissions in shallow lakes. Often, CH_4 ebullition rates are compared with CH_4 diffusion rates only when bubbles occur, omitting the periods of zero ebullition when calculating ebullition rates, or even neglecting the CH_4 ebullition in the CH_4 budget, as in Soja et al. (2014). In addition, ebullition rates are sometimes measured with very short closure period (minutes-hours) and not continuously. These short-term measurements are often up-scaled to estimate ebullition rates over longer time periods. However, for a more accurate assessment of the significance of CH_4 release via bubbles, longer closure periods and extended measurement periods are required, ideally covering an entire season or even a full year. Omitting instances of zero CH_4 ebullition rates from the calculation of CH_4 emissions might result in an overestimation of the contribution of the ebullition pathway. In our study, we identified instances of zero CH_4 ebullition rates in 12 % of the observations (and included them in the ebullition flux estimates), whereas Soja et al. (2014) did not observe ebullition in 60 % of their measurements.

Some studies consider the ebullition pathway for CH_4 fluxes of lakes to be more dominant than the diffusion pathway (Bastviken et al., 2011; Aben et al., 2017), or at least to play a significant role (Soja et al., 2014; DelSontro et al., 2016). Camacho et al. (2017) studied CH_4 emissions, included ebullition but not measuring it with distinct methodologies, of saline lakes in Spain, having conductivity values higher than 7.2 mS cm^{-1}, which are higher and, therefore, maybe not comparable to conductivity values of subsaline lakes such as Lake Neusiedl (see Fig. S10B). Nevertheless, their CH_4 emission increased by 30–50 % when adding ebullition to diffusion. One potential subsaline lake site (conductivity 1–3 mS cm^{-1}) in the study of Wang et al. (2021b) showed on average slightly lower ebullition contribution (47 %) compared to diffusion, whereas all other lake sites had on average a dominance of the ebullition pathway. This example confirms that not all lake ecosystems behave in the same way and highlights the need for more accurate ebullition measurements to better understand and assess these systems.

Our study demonstrates that, on average and cumulatively, from March to July 2021, the diffusion pathway of CH_4 flux dominates over the ebullition pathway in two out of three locations at Lake Neusiedl (OW and CH). In contrast, the RB location at Lake Neusiedl presents a more complex scenario: the median CH_4 flux of the ebullition pathway was smaller than that of the diffusion pathway, whereas the mean values showed the opposite trend. Nonetheless, at this location, the mean values of the two pathways showed non-significant differences from each other. Additionally, at this location, the highest and lowest CH_4 flux rates were measured through the ebullition pathway. Cumulatively over the measurement period, from March to July 2021, both transport pathways at RB showed no significant difference. Further unraveling this complexity at the RB location would require more extensive ebullition measurements in the future, as this matter cannot be definitively addressed solely with the current findings at Lake Neusiedl.

5. Conclusions

Our study demonstrated a clear heterogeneity in CH_4 ebullition rates over both time (from March to July 2021) and space (locations) at Lake Neusiedl. By studying just three locations within the lake, not too far away from each other, we were able to observe the substantial influence of lake characteristics on CH_4 emission rates, particularly affecting the ebullition pathway. Thereby, the ebullition rates of distinct ecosystems within a lake should not be considered homogeneous due to the spatial differences in the influencing factors such as temperature, water level, and organic carbon, which strongly impact ebullition rates. Even though ebullition rates vary significantly within the lake, the dominant type of methanogenesis (acetoclastic) remains consistent throughout the lake.

The prevalence of the ebullition pathway over diffusion pathway, or vice versa, can vary considerably across different sites within a lake. In two out of three locations at Lake Neusiedl, an example for a subsaline lake, ebullition is not more important as CH_4 emission pathway than diffusion, whereas at one location, the two emission pathways are almost equally important.

Funding

Open access funding provided by the University of Vienna.

CRediT authorship contribution statement

Pamela Alessandra Baur: Data curation, Methodology, Formal analysis, Visualization, Conceptualization, Writing – original draft, Writing – review & editing, Investigation, Software, Validation. **Daniela Henry Pinilla:** Data curation, Formal analysis, Investigation, Writing – review & editing. **Stephan Glatzel:** Resources, Conceptualization, Funding acquisition, Project administration, Supervision, Writing – review & editing.

Declaration of competing interest

The authors declare no conflict of interest.

Data availability

The data generated during this study are available at the Phaidra repository of the University of Vienna under https://doi.org/10.25365/phaidra.424.

Acknowledgements

We highly acknowledge the support of the Biological Station Lake Neusiedl (Illmitz, Austria) and the National Park Neusiedler See Seewinkel for access to the study area, provision of permits, and friendly cooperation. We thank the regional government of Land Burgenland for issuing the exceptional permit ("Naturschutzbehördliche Ausnahmegenehmigung") for entering the National Park nature zone and conducting research there. We thank the Geoecology team for their support in the field and in the lab.

Appendix A. Supplementary data

Supplementary data to this article can be found online at https://doi.org/10.1016/j.scitotenv.2023.169112.

References

Aben, R.C.H., Barros, N., van Donk, E., Frenken, T., Hilt, S., Kazanjian, G., Lamers, L.P. M., Peeters, E.T.H.M., Roelofs, J.G.M., de Senerpont Domis, L.N., Stephan, S., Velthuis, M., van de Waal, D.B., Wik, M., Thornton, B.F., Wilkinson, J., DelSontro, T., Kosten, S., 2017. Cross continental increase in methane ebullition under climate change. Nat. Commun. 8, 1682. https://doi.org/10.1038/s41467-017-01535-y.

Aguirrezabala-Campano, T., Gerardo-Nieto, O., Gonzalez-Valencia, R., Souza, V., Thalasso, F., 2019. Methane dynamics in the subsaline ponds of the Chihuahuan Desert: a first assessment. Sci. Total Environ. 666, 1255–1264. https://doi.org/10.1016/j.scitotenv.2019.02.163.

Alin, S.R., Johnson, T.C., 2007. Carbon cycling in large lakes of the world: a synthesis of production, burial, and lake-atmosphere exchange estimates. Glob. Biogeochem. Cycles 21, GB3002. https://doi.org/10.1029/2006GB002881.

Armstrong, J., Armstrong, W., 1990. Light-enhanced convective throughflow increases oxygenation in rhizomes and rhizosphere of phragmites australis (cav.) trin. ex steud. New Phytol. 114, 121–128. https://doi.org/10.1111/j.1469-8137.1990.tb00382.x.

Auguie, B., 2017. gridExtra: miscellaneous functions for "grid" graphics. URL: https://CRAN.R-project.org/package=gridExtra. r package version 2.3.

Bartosiewicz, M., Laurion, I., MacIntyre, S., 2015. Greenhouse gas emission and storage in a small shallow lake. Hydrobiologia 757, 101–115. https://doi.org/10.1007/s10750-015-2240-2.

Bastviken, D., Ejlertsson, J., Tranvik, L., 2002. Measurement of methane oxidation in lakes: a comparison of methods. Environ. Sci. Technol. 36, 3354–3361. https://doi.org/10.1021/es010311p.

Bastviken, D., Cole, J.J., Pace, M.L., van de Bogert, M.C., 2008. Fates of methane from different lake habitats: connecting whole-lake budgets and ch 4 emissions. J. Geophys. Res. Biogeosci. 113, G02024 https://doi.org/10.1029/2007JG000608.

Bastviken, D., Tranvik, L.J., Downing, J.A., Crill, P.M., Enrich-Prast, A., 2011. Freshwater methane emissions offset the continental carbon sink. Science (New York, N.Y.) 331, 50. https://doi.org/10.1126/science.1196808.

Baty, F., Ritz, C., Charles, S., Brutsche, M., Flandrois, J.P., Delignette-Muller, M.L., 2015. A toolbox for nonlinear regression in R: the package nlstools. J. Stat. Softw. 66, 1–21. https://doi.org/10.18637/jss.v066.i05.

Bogard, M.J., del Giorgio, P.A., Boutet, L., Chaves, M.C.G., Prairie, Y.T., Merante, A., Derry, A.M., 2014. Oxic water column methanogenesis as a major component of aquatic ch4 fluxes. Nat. Commun. 5, 5350. https://doi.org/10.1038/ncomms6350.

Boguski, T.K., 2006. Understanding units of measurement. Environmental Science and Technology Briefs for Citizens, 2 p. URL: https://engg.k-state.edu/chsr/outreach/resources/docs/measure.pdf.

Boros, E., Horváth, Z., Wolfram, G., Vörös, L., 2014. Salinity and ionic composition of the shallow astatic soda pans in the Carpathian Basin. Ann. Limnol. Int. J. Limnol. 50, 59–69. https://doi.org/10.1051/limn/2013068.

van den Brand, T., 2023. ggh4x: hacks for 'ggplot2'. URL: https://CRAN.R-project.org/package=ggh4x.

Buchsteiner, C., Baur, P.A., Glatzel, S., 2023. Spatial analysis of intra-annual reed ecosystem dynamics at lake neusiedl using rgb drone imagery and deep learning. Remote Sens. 15, 3961. https://doi.org/10.3390/rs15163961.

Butterbach-Bahl, K., Kiese, R., Liu, C., 2011. Measurements of biosphere-atmosphere exchange of CH_4 in terrestrial ecosystems. Methods Enzymol. 495, 271–287. https://doi.org/10.1016/B978-0-12-386905-0.00018-8.

Camacho, A., Picazo, A., Rochera, C., Santamans, A., Morant, D., Miralles-Lorenzo, J., Castillo-Escrivà, A., 2017. Methane emissions in Spanish saline lakes: current rates, temperature and salinity responses, and evolution under different climate change scenarios. Water 9, 659. https://doi.org/10.3390/w9090659.

Chanton, J.P., 2005. The effect of gas transport on the isotope signature of methane in wetlands. Org. Geochem. 36, 753–768. https://doi.org/10.1016/j.orggeochem.2004.10.007.

Cohen, J., 1988. Statistical Power Analysis for the Behavioral Sciences, 2nd edition. Taylor and Francis, Hoboken. https://doi.org/10.4324/9780203771587.

Conrad, R., 2005. Quantification of methanogenic pathways using stable carbon isotopic signatures: a review and a proposal. Org. Geochem. 36, 739–752. https://doi.org/10.1016/j.orggeochem.2004.09.006.

Conrad, R., 2009. The global methane cycle: recent advances in understanding the microbial processes involved. Environ. Microbiol. Rep. 1, 285–292. https://doi.org/10.1111/j.1758-2229.2009.00038.x.

Conrad, R., 2020. Importance of hydrogenotrophic, aceticlastic and methylotrophic methanogenesis for methane production in terrestrial, aquatic and other anoxic environments: a mini review. Pedosphere 30, 25–39. https://doi.org/10.1016/S1002-0160(18)60052-9.

Csaplovics, E., 2019. Der Schilfgürtel des Neusiedler Sees. Österreichische Wasser- und Abfallwirtschaft 71, 494–507. https://doi.org/10.1007/s00506-019-00622-2.

Davidson, T.A., Audet, J., Jeppesen, E., Landkildehus, F., Lauridsen, T.L., Søndergaard, M., Syväranta, J., 2018. Synergy between nutrients and warming enhances methane ebullition from experimental lakes. Nat. Clim. Chang. 8, 156–160. https://doi.org/10.1007/978-94-007-4001-3_197.

DelSontro, T., Boutet, L., St-Pierre, A., del Giorgio, P.A., Prairie, Y.T., 2016. Methane ebullition and diffusion from northern ponds and lakes regulated by the interaction between temperature and system productivity. Limnol. Oceanogr. 61, S62–S77. https://doi.org/10.1002/lno.10335.

DelSontro, T., Beaulieu, J.J., Downing, J.A., 2018. Greenhouse gas emissions from lakes and impoundments: upscaling in the face of global change. Limnol. Oceanogr. Lett. 3, 64–75. https://doi.org/10.1002/lol2.10073.

Dowle, M., Srinivasan, A., 2023. data.table: extension of 'data.frame'. URL: https://CRAN.R-project.org/package=data.table. r package version 1.14.8.

Encinas Fernández, J., Peeters, F., Hofmann, H., 2016. On the methane paradox: transport from shallow water zones rather than in situ methanogenesis is the major source of CH4 in the open surface water of lakes. J. Geophys. Res. Biogeosci. 121, 2717–2726. https://doi.org/10.1002/2016JG003586.

Flury, S., McGinnis, D.F., Gessner, M.O., 2010. Methane emissions from a freshwater marsh in response to experimentally simulated global warming and nitrogen enrichment. J. Geophys. Res. 115 https://doi.org/10.1029/2009JG001079.

Gagolewski, M., 2022. stringi: fast and portable character string processing in R. J. Stat. Softw. 103 https://doi.org/10.18637/jss.v103.i02.

Gardolinski, P.C., Hanrahan, G., Achterberg, E.P., Gledhill, M., Tappin, A.D., House, W. A., Worsfold, P.J., 2001. Comparison of sample storage protocols for the determination of nutrients in natural waters. Water Res. 35, 3670–3678. https://doi.org/10.1016/S0043-1354(01)00088-4.

Gupta, H.V., Kling, H., Yilmaz, K.K., Martinez, G.F., 2009. Decomposition of the mean squared error and NSE performance criteria: implications for improving hydrological modelling. J. Hydrol. 377, 80–91. https://doi.org/10.1016/j.jhydrol.2009.08.003.

Hackl, P., Ledolter, J., 2023. A statistical analysis of the water levels at Lake Neusiedl. Austrian J. Stat. 52, 87–100. https://doi.org/10.17713/ajs.v52i1.1444.

Hammer, U.T., 1986. Saline lake ecosystems of the world. Monographiae Biologicae 59. Junk, Dordrecht [et al.].

Happell, J.D., Chanton, J.P., Showers, W.S., 1994. The influence of methane oxidation on the stable isotopic composition of methane emitted from florida swamp forests. Geochim. Cosmochim. Acta 58, 4377–4388. https://doi.org/10.1016/0016-7037(94)90341-7.

Hoffmann, M., Schulz-Hanke, M., Garcia Alba, J., Jurisch, N., Hagemann, U., Sachs, T., Sommer, M., Augustin, J., 2017. A simple calculation algorithm to separate high-resolution ch4 flux measurements into ebullition- and diffusion-derived components. Atmos. Meas. Tech. 10, 109–118. https://doi.org/10.5194/amt-10-109-2017.

Hope, R.M., 2022. Rmisc: ryan miscellaneous. URL: https://CRAN.R-project.org/package=Rmisc. r package version 1.5.1.

Johnson, M.S., Matthews, E., Du, J., Genovese, V., Bastviken, D., 2022. Methane emission from global lakes: new spatiotemporal data and observation-driven modeling of methane dynamics indicates lower emissions. J. Geophys. Res. Biogeosci. 127, e2022JG006793 https://doi.org/10.1029/2022JG006793.

Käki, T., Ojala, A., Kankaala, P., 2001. Diel variation in methane emissions from stands of phragmites australis (cav.) trin. ex steud. and typha latifolia l. in a boreal lake. Aquat. Bot. 71, 259–271. https://doi.org/10.1016/S0304-3770(01)00186-3.

Kandeler, E., Gerber, H., 1988. Short-term assay of soil urease activity using colorimetric determination of ammonium. Biol. Fertil. Soils 6, 68–72. https://doi.org/10.1007/BF00257924.

Kassambara, A., 2023a. ggpubr: 'ggplot2' based publication ready plots. URL: https://CRAN.R-project.org/package=ggpubr.

Kassambara, A., 2023b. rstatix: pipe-friendly framework for basic statistical tests. URL: https://CRAN.R-project.org/package=rstatix. r package version 0.7.2.

Kleint, J.F., Wellach, Y., Schroll, M., Keppler, F., Isenbeck-Schröter, M., 2021. The impact of seasonal sulfate–methane transition zones on methane cycling in a sulfate–enriched freshwater environment. Limnol. Oceanogr. 66, 2290–2308. https://doi.org/10.1002/lno.11754.

Langenegger, T., Vachon, D., Donis, D., McGinnis, D.F., 2019. What the bubble knows: lake methane dynamics revealed by sediment gas bubble composition. Limnol. Oceanogr. 64, 1526–1544. https://doi.org/10.1002/lno.11133.

Li, M., Peng, C., Zhu, Q., Zhou, X., Yang, G., Song, X., Zhang, K., 2020. The significant contribution of lake depth in regulating global lake diffusive methane emissions. Water Res. 172, 115465 https://doi.org/10.1016/j.watres.2020.115465.

Linkhorst, A., Hiller, C., DelSontro, T.M., Azevedo, G., Barros, N., Mendonça, R., Sobek, S., 2020. Comparing methane ebullition variability across space and time in a brazilian reservoir. Limnol. Oceanogr. 65, 1623–1634. https://doi.org/10.1002/lno.11410.

Lovley, D.R., Klug, M.J., 1983. Sulfate reducers can outcompete methanogens at freshwater sulfate concentrations. Appl. Environ. Microbiol. 45, 187–192. https://doi.org/10.1128/aem.45.1.187-192.1983.

Männistö, E., Korrensalo, A., Alekseychik, P., Mammarella, I., Peltola, O., Vesala, T., Tuittila, E.S., 2019. Multi-year methane ebullition measurements from water and bare peat surfaces of a patterned boreal bog. Biogeosciences 16, 2409–2421. https://doi.org/10.5194/bg-16-2409-2019.

McClure, R.P., Lofton, M.E., Chen, S., Krueger, K.M., Little, J.C., Carey, C.C., 2020. The magnitude and drivers of methane ebullition and diffusion vary on a longitudinal gradient in a small freshwater reservoir. J. Geophys. Res. Biogeosci. 125 https://doi.org/10.1029/2019JG005205.

Messager, M.L., Lehner, B., Grill, G., Nedeva, I., Schmitt, O., 2016. Estimating the volume and age of water stored in global lakes using a geo-statistical approach. Nat. Commun. 7, 13603. https://doi.org/10.1038/ncomms13603.

Miller, B.L., Holtgrieve, G.W., Arias, M.E., Uy, S., Chheng, P., 2022. Coupled ch4 production and oxidation support co2 supersaturation in a tropical flood pulse lake (Tonle Sap Lake, Cambodia). Proc. Natl. Acad. Sci. U. S. A. 119 https://doi.org/10.1073/pnas.2107667119.

Miranda, K.M., Espey, M.G., Wink, D.A., 2001. A rapid, simple spectrophotometric method for simultaneous detection of nitrate and nitrite. Nitric Oxide 5, 62–71. https://doi.org/10.1006/niox.2000.0319.

Murphy, J.A.M.E.S., Riley, J.P., 1962. A modified single solution method for the determination of phosphate in natural waters. Anal. Chim. Acta 27, 31–36. https://doi.org/10.1016/S0003-2670(00)88444-5.

Neubauer, S.C., Megonigal, J.P., 2015. Moving beyond global warming potentials to quantify the climatic role of ecosystems. Ecosystems 18, 1000–1013. https://doi.org/10.1007/s10021-015-9879-4.

Patil, I., 2021. Visualizations with statistical details: the 'ggstatsplot' approach. J. Open Source Softw. 6, 3167. https://doi.org/10.21105/joss.03167.
Peeters, F., Encinas Fernandez, J., Hofmann, H., 2019. Sediment fluxes rather than oxic methanogenesis explain diffusive ch4 emissions from lakes and reservoirs. Sci. Rep. 9, 243. https://doi.org/10.1038/s41598-018-36530-w.
Pi, X., Luo, Q., Feng, L., Xu, Y., Tang, J., Liang, X., Ma, E., Cheng, R., Fensholt, R., Brandt, M., Cai, X., Gibson, L., Liu, J., Zheng, C., Li, W., Bryan, B.A., 2022. Mapping global lake dynamics reveals the emerging roles of small lakes. Nat. Commun. 13, 5777. https://doi.org/10.1038/s41467-022-33239-3.
Poffenbarger, H.J., Needelman, B.A., Megonigal, J.P., 2011. Salinity influence on methane emissions from tidal marshes. Wetlands 31, 831–842. https://doi.org/10.1007/s13157-011-0197-0.
R Core Team, 2021. R: A Language and Environment for Statistical Computing. R Foundation for Statistical Computing, Vienna, Austria. URL: https://www.R-project.org/.
Reif, D., Zoboli, O., Wolfram, G., Amann, A., Saracevic, E., Riedler, P., Hainz, R., Hintermaier, S., Krampe, J., Zessner, M., 2022. Pollutant source or sink? Adsorption and mobilization of pfos and pfoa from sediments in a large shallow lake with extended reed belt. J. Environ. Manag. 320, 115871 https://doi.org/10.1016/j.jenvman.2022.115871.
Rochette, P., Ellert, B., Gregorich, E.G., Desjardins, R.L., Pattey, E., Lessard, R., Johnson, B.G., 1997. Description of a dynamic closed chamber for measuring soil respiration and its comparison with other techniques. Can. J. Soil Sci. 77, 195–203. https://doi.org/10.4141/S96-110.
Rosentreter, J.A., Borges, A.V., Deemer, B.R., Holgerson, M.A., Liu, S., Song, C., Melack, J., Raymond, P.A., Duarte, C.M., Allen, G.H., Olefeldt, D., Poulter, B., Battin, T.I., Eyre, B.D., 2021. Half of global methane emissions come from highly variable aquatic ecosystem sources. Nat. Geosci. 14, 225–230. https://doi.org/10.1038/s41561-021-00715-2.
Saunois, M., Stavert, A.R., Poulter, B., Bousquet, P., Canadell, J.G., Jackson, R.B., Raymond, P.A., Dlugokencky, E.J., Houweling, S., Patra, P.K., Ciais, P., Arora, V.K., Bastviken, D., Bergamaschi, P., Blake, D.R., Brailsford, G., Bruhwiler, L., Carlson, K.M., Carrol, M., Castaldi, S., Chandra, N., Crevoisier, C., Crill, P.M., Covey, K., Curry, C.L., Etiope, G., Frankenberg, C., Gedney, N., Hegglin, M.I., Höglund-Isaksson, L., Hugelius, G., Ishizawa, M., Ito, A., Janssens-Maenhout, G., Jensen, K.M., Joos, F., Kleinen, T., Krummel, P.B., Langenfelds, R.L., Laruelle, G.G., Liu, L., Machida, T., Maksyutov, S., McDonald, K.C., McNorton, J., Miller, P.A., Melton, J.R., Morino, I., Müller, J., Murguia-Flores, F., Naik, V., Niwa, Y., Noce, S., O'Doherty, S., Parker, R.J., Peng, C., Peng, S., Peters, G.P., Prigent, C., Prinn, R., Ramonet, M., Regnier, P., Riley, W.J., Rosentreter, J.A., Segers, A., Simpson, I.J., Shi, H., Smith, S.J., Steele, L.P., Thornton, B.F., Tian, H., Tohjima, Y., Tubiello, F.N., Tsuruta, A., Viovy, N., Voulgarakis, A., Weber, T.S., van Weele, M., van der Werf, G.R., Weiss, R.F., Worthy, D., Wunch, D., Yin, Y., Yoshida, Y., Zhang, W., Zhang, Z., Zhao, Y., Zheng, B., Zhu, Q., Zhu, Q., Zhuang, Q., 2020. The global methane budget 2000–2017. Earth Syst. Sci. Data 12, 1561–1623. https://doi.org/10.5194/essd-12-1561-2020.
Schenk, J., Sawakuchi, H.O., Sieczko, A.K., Pajala, G., Rudberg, D., Hagberg, E., Fors, K., Laudon, H., Karlsson, J., Bastviken, D., 2021. Methane in lakes: variability in stable carbon isotopic composition and the potential importance of groundwater input. Front. Earth Sci. 9 https://doi.org/10.3389/feart.2021.722215.
Schmiedeskamp, M., Praetzel, L.S.E., Bastviken, D., Knorr, K.H., 2021. Whole–lake methane emissions from two temperate shallow lakes with fluctuating water levels: relevance of spatiotemporal patterns. Limnol. Oceanogr. 66, 2455–2469. https://doi.org/10.1002/lno.11764.
Sø, J.S., Sand-Jensen, K., Martinsen, K.T., Polauke, E., Kjær, J.E., Reitzel, K., Kragh, T., 2023. Methane and carbon dioxide fluxes at high spatiotemporal resolution from a small temperate lake. Sci. Total Environ. 878, 162895 https://doi.org/10.1016/j.scitotenv.2023.162895.
Soja, G., Züger, J., Knoflacher, M., Kinner, P., Soja, A.M., 2013. Climate impacts on water balance of a shallow steppe lake in eastern Austria (lake neusiedl). J. Hydrol. 480, 115–124. https://doi.org/10.1016/j.jhydrol.2012.12.013.
Soja, G., Kitzler, B., Soja, A.M., 2014. Emissions of greenhouse gases from lake neusiedl, a shallow steppe lake in eastern Austria. Hydrobiologia 731, 125–138. https://doi.org/10.1007/s10750-013-1681-8.
Ström, L., Ekberg, A., Mastepanov, M., Røjle Christensen, T., 2003. The effect of vascular plants on carbon turnover and methane emissions from a tundra wetland. Glob. Chang. Biol. 9, 1185–1192. https://doi.org/10.1046/j.1365-2486.2003.00655.x.
Ström, L., Mastepanov, M., Christensen, T.R., 2005. Species-specific effects of vascular plants on carbon turnover and methane emissions from wetlands. Biogeochemistry 75, 65–82. https://doi.org/10.1007/s10533-004-6124-1.
Thottathil, S.D., Prairie, Y.T., 2021. Coupling of stable carbon isotopic signature of methane and ebullitive fluxes in northern temperate lakes. Sci. Total Environ. 777, 146117 https://doi.org/10.1016/j.scitotenv.2021.146117.
Tolotti, M., Guella, G., Herzig, A., Rodeghiero, M., Rose, N.L., Soja, G., Zechmeister, T., Yang, H., Teubner, K., 2021. Assessing the ecological vulnerability of the shallow steppe lake neusiedl (Austria-Hungary) to climate-driven hydrological changes using a palaeolimnological approach. J. Great Lakes Res. https://doi.org/10.1016/j.jglr.2021.06.004.
U.S.EPA, 1999. Test methods for evaluating solid waste physical/chemical methods. In: Method 9038: Sulfate (Turbidimetric). U.S. Environmental Protection Agency (SW-846).
Wang, C., Tong, C., Chambers, L.G., Liu, X., 2017. Identifying the salinity thresholds that impact greenhouse gas production in subtropical tidal freshwater marsh soils. Wetlands 37, 559–571. https://doi.org/10.1007/s13157-017-0890-8.
Wang, G., Xia, X., Liu, S., Zhang, L., Zhang, S., Wang, J., Xi, N., Zhang, Q., 2021a. Intense methane ebullition from urban inland waters and its significant contribution to greenhouse gas emissions. Water Res. 189, 116654 https://doi.org/10.1016/j.watres.2020.116654.
Wang, L., Du, Z., Wei, Z., Xu, Q., Feng, Y., Lin, P., Lin, J., Chen, S., Qiao, Y., Shi, J., Xiao, C., 2021b. High methane emissions from thermokarst lakes on the tibetan plateau are largely attributed to ebullition fluxes. Sci. Total Environ. 801, 149692 https://doi.org/10.1016/j.scitotenv.2021.149692.
Whiticar, M.J., 1999. Carbon and hydrogen isotope systematics of bacterial formation and oxidation of methane. Chem. Geol. 161, 291–314. https://doi.org/10.1016/S0009-2541(99)00092-3.
Whiticar, M.J., Faber, E., 1986. Methane oxidation in sediment and water column environments—isotope evidence. Org. Geochem. 10, 759–768. https://doi.org/10.1016/S0146-6380(86)80013-4.
Whiticar, M., Faber, E., Schoell, M., 1986. Biogenic methane formation in marine and freshwater environments: Co2 reduction vs. acetate fermentation—isotope evidence. Geochim. Cosmochim. Acta 50, 693–709. https://doi.org/10.1016/0016-7037(86)90346-7.
Wickham, H., 2016. ggplot2: Elegant Graphics for Data Analysis. Springer-Verlag, New York. URL: https://ggplot2.tidyverse.org.
Wickham, H., Averick, M., Bryan, J., Chang, W., McGowan, L., François, R., Grolemund, G., Hayes, A., Henry, L., Hester, J., Kuhn, M., Pedersen, T., Miller, E., Bache, S., Müller, K., Ooms, J., Robinson, D., Seidel, D., Spinu, V., Takahashi, K., Vaughan, D., Wilke, C., Woo, K., Yutani, H., 2019. Welcome to the tidyverse. J. Open Source Softw. 4, 1686. https://doi.org/10.21105/joss.01686.
Wik, M., Crill, P.M., Varner, R.K., Bastviken, D., 2013. Multiyear measurements of ebullitive methane flux from three subarctic lakes. J. Geophys. Res. Biogeosci. 118, 1307–1321. https://doi.org/10.1002/jgrg.20103.
Wik, M., Thornton, B.F., Bastviken, D., Macintyre, S., Varner, R.K., Crill, P.M., 2014. Energy input is primary controller of methane bubbling in subarctic lakes. Geophys. Res. Lett. 41, 555–560. https://doi.org/10.1002/2013GL058510.
Wik, M., Thornton, B.F., Bastviken, D., Uhlbäck, J., Crill, P.M., 2016. Biased sampling of methane release from northern lakes: a problem for extrapolation. Geophys. Res. Lett. 43, 1256–1262. https://doi.org/10.1002/2015GL066501.
Wik, M., Thornton, B.F., Varner, R.K., McCalley, C., Crill, P.M., 2020. Stable methane isotopologues from northern lakes suggest that ebullition is dominated by sub–lake scale processes. J. Geophys. Res. Biogeosci. 125 https://doi.org/10.1029/2019JG005601.
Wilkinson, J., Bodmer, P., Lorke, A., 2019. Methane dynamics and thermal response in impoundments of the Rhine River, Germany. Sci. Total Environ. 659, 1045–1057. https://doi.org/10.1016/j.scitotenv.2018.12.424.
Wolfram, G., Herzig, A., 2013. Nährstoffbilanz neusiedler see. Wiener Mitteilungen 317–338.
Worsfold, P.J., Gimbert, L.J., Mankasingh, U., Omaka, O.N., Hanrahan, G., Gardolinski, P.C., Haygarthd, P.M., Turnere, B.L., Keith-Roach, M.J., McKelvie, I.D., 2005. Sampling, sample treatment and quality assurance issues for the determination of phosphorus species in natural waters and soils. Talanta 66, 273–293. https://doi.org/10.1016/j.talanta.2004.09.006.
Wurtsbaugh, W.A., Miller, C., Null, S.E., DeRose, R.J., Wilcock, P., Hahnenberger, M., Howe, F., Moore, J., 2017. Decline of the world's saline lakes. Nat. Geosci. 10, 816–821. https://doi.org/10.1038/ngeo3052.
Yamamoto, S., Alcauskas, J.B., Crozier, T.E., 1976. Solubility of methane in distilled water and seawater. J. Chem. Eng. Data 21, 78–80. https://doi.org/10.1021/je60068a029.
Yao, F., Livneh, B., Rajagopalan, B., Wang, J., Crétaux, J.F., Wada, Y., Berge-Nguyen, M., 2023. Satellites reveal widespread decline in global lake water storage. Science 380, 743–749. https://doi.org/10.1126/science.abo2812.
Yvon-Durocher, G., Allen, A.P., Bastviken, D., Conrad, R., Gudasz, C., St-Pierre, A., Thanh-Duc, N., del Giorgio, P.A., 2014. Methane fluxes show consistent temperature dependence across microbial to ecosystem scales. Nature 507, 488–491. https://doi.org/10.1038/nature13164.
Zambrano-Bigiarini, Mauricio, 2020. hydroGOF: Goodness-of-fit Functions for Comparison of Simulated and Observed Hydrological Time Series. https://doi.org/10.5281/zenodo.839854 r package version 0.4-0.
Zheng, Y., Wu, S., Xiao, S., Yu, K., Fang, X., Xia, L., Wang, J., Liu, S., Freeman, C., Zou, J., 2022. Global methane and nitrous oxide emissions from inland waters and estuaries. Glob. Chang. Biol. 28, 4713–4725. https://doi.org/10.1111/gcb.16233.
Zoboli, O., Hainz, R., Riedler, P., Kum, G., Sigmund, E., Hintermaier, S., Saracevic, E., Krampe, J., Zessner, M., Wolfram, G., 2023. Fate of nutrients and trace contaminants in a large shallow soda lake. Spatial gradients and underlying processes from the tributary river to the reed belt. Environ Sci Process Impacts 25, 1505–1518. https://doi.org/10.1039/d3em00152k.